



A process-based model of nitrogen cycling in forest plantations Part II. Simulating growth and nitrogen mineralisation of *Eucalyptus globulus* plantations in south-western Australia

M. Corbeels^{a,b,*}, R.E. McMurtrie^c, D.A. Pepper^c, A.M. O'Connell^a

^a CSIRO Forestry and Forest Products, Private Bag 5, Wembley, WA 6913, Australia

^b UMR System, Centre de coopération internationale en recherche agronomique pour le développement (CIRAD),
Avenue Agropolis, 34398 Montpellier Cedex 5, France

^c School of Biological, Earth and Environmental Sciences, University of New South Wales, Sydney, NSW 2052, Australia

Received 11 August 2004; received in revised form 22 June 2005; accepted 6 July 2005

Abstract

We applied a new version of the G'DAY ecosystem model to short-rotation plantations of *Eucalyptus globulus* growing under a Mediterranean climate in south-western Australia. The new version, that includes modified submodels for biomass production, water balance, litter and soil organic matter (SOM) decomposition, and soil inorganic N balance, was parameterised and applied to three experimental eucalypt sites (Mumballup, Darkan and Northcliffe) of contrasting productivity. With a common base set of parameter values, the model was able to correctly reproduce observed time series of soil water content, canopy leaf area index and stemwood data at the three sites. The model's ability to simulate soil N supply under forest plantations was tested by simulating N mineralisation at each of the three sites over the duration of the experiment (10 years). Simulated annual net N mineralisation in the litter and top 20 cm soil layer ranged from 50 to 170 kg N ha⁻¹ across the sites as a result of differences in rates of litter production, SOM and litter decomposition, and microbial N immobilisation and (re-)mineralisation. Simulations of annual soil N mineralisation were similar to measured rates over a 3-year period, except for an overestimation in 1 year at Mumballup and 2 years at Darkan. Model results indicated the importance of fine root production and turnover for N supply. As plantations age, supply of N to trees increasingly originates from litter decomposition, while the contribution from decomposition of SOM decreases. Although major soil feedbacks associated with litter production, decomposition and N availability are adequately integrated into G'DAY, further work is required in some aspects of the model, including the utility of the C-allocation submodel over a wide range of site conditions and silvicultural treatments.

© 2005 Elsevier B.V. All rights reserved.

Keywords: C and N cycling; *Eucalyptus* plantation; G'DAY model; N mineralisation; Simulation modelling

* Corresponding author. Present address: CIRAD-Ca, EMBRAPA-Cerrados, Km 18, BR 020, CP 08223, 73301-970, Planaltina, DF, Brazil.
Tel.: +55 61 388 98 49; fax: +55 61 388 98 79.

E-mail address: Marc.corbeels@cirad.fr (M. Corbeels).

1. Introduction

Process-based simulation models are a powerful tool for studying the functioning of forest ecosystems and their processes (e.g. Aber et al., 1982; Sands et al., 2000). Increasingly, they are used to gain a better understanding of the effects of silvicultural practices (e.g. fertilisation, harvest residue management, stocking density and thinning) on plantation productivity (Almeida et al., 2004; Battaglia et al., 2004; Corbeels et al., 2005a). Modelling of carbon (C) and nitrogen (N) cycling is particularly important for short-rotation forest plantations because N frequently limits their C production (e.g. Bernhard-Reversat, 1996; Agus et al., 2004; O'Connell et al., 2004; Smethurst et al., 2004). It is a major challenge to modellers because of complex interactions between C and N cycling, including feedbacks between plant and soil that are associated with litter production, organic matter decomposition and soil N availability (Scott and Binkley, 1997; Campbell and Gower, 2000). Integrating plant–soil feedbacks into forest-ecosystem models is, however, essential, if one wants to analyse how silvicultural operations such as harvest residue management affect forest yield through their impact on soil fertility (King, 1996; Rolff and Ågren, 1999). For example, Corbeels et al. (2005a) modelled the link between soil N fertility and productivity for eucalypt plantations under various options of harvest residue and N management. They showed that a plant–soil model with internal C and N cycles is required for predicting sustainable wood yield over multiple rotations. Besides, a successful forest-ecosystem model needs to be well-balanced, describing plant physiological and soil biogeochemical processes in comparable levels of detail.

Over the last two decades there has been considerable progress in the development of various kinds of process-based forest growth models (e.g. see review by Mäkelä et al., 2000). However, these models differ considerably in terms of structure, processes incorporated, formulation of individual processes and nature of driving variables. As a result, when various models are applied to a single site, their outputs may be widely different. For example, following calibration of a number of leading ecosystem models to several years of field data, the coefficient of variation in predicted annual soil N mineralisation for a specific year under a *Pinus*

radiata plantation in eastern Australia was greater than 40% (Ryan et al., 1996).

Generic Decomposition And Yield (G'DAY) (Comins and McMurtrie, 1993; Medlyn et al., 2000; McMurtrie et al., 2001) is a relatively simple, process-based ecosystem model of C and N cycling that links a plant production model (McMurtrie and Wolf, 1983; McMurtrie, 1991; Medlyn et al., 2000) to the decomposition submodel of CENTURY (Parton et al., 1987, 1993). It is a generic model in the sense that its structure and the underlying concepts are not site or species specific, but it must be parameterised for individual sites and species. It uses a daily time step with inputs of daily meteorological data for incoming total short-wave radiation, precipitation and minimum and maximum air temperatures. The G'DAY version with CENTURY (henceforth referred to as G'DAY-Century) has been applied to several forest and grassland experiments for investigating plant growth responses to climate change (Medlyn et al., 2000; McMurtrie et al., 2001; Pepper et al., 2005), age-related decline in forest production (Murty and McMurtrie, 2000), impacts of land-use change on soil C storage (Halliday et al., 2003), and effects of management practices on sustained productivity (McMurtrie et al., 2001). Each of these studies concluded that there is a need to improve the representation of soil C and N cycles in G'DAY-Century, which led to the development of a new organic matter decomposition submodel that advances the mechanistic treatment of the N mineralisation-immobilisation process during decomposition of litter and soil organic matter (SOM). This new decomposition model has been described and tested in a companion paper (Corbeels et al., 2005b), and was proven to simulate more accurately N mineralisation-immobilisation dynamics in decomposing *Eucalyptus globulus* residues compared to G'DAY-Century (see Fig. 4 in Corbeels et al., 2005b).

The objective of this paper was to present a model of C and N cycling for fast-growing forest plantations that would allow us to simulate feedbacks between site N fertility and plantation productivity over the long-term and address sustainability issues of silvicultural management. The paper is structured as follows. In Section 2, we describe the updated version of G'DAY for C and N cycling in fast-growing forest plantations and in Section 3 the available experimental data. In Section 4, we parameterise the new model for three *E. globulus* ssp. *globulus* plantations in south-western

Australia, and in Section 5, we evaluate model predictions of soil N mineralisation against measurements for these eucalypt stands. In Section 6, we analyse parameter sensitivity and identifiability in relation to available measurements. In Section 7, the main results are discussed, and in Section 8 conclusions are drawn. The application of this updated version of the G'DAY model to long-term productivity of eucalypt plantations in relation to site N fertility can be found in Corbeels et al. (2005a).

There were several motivations for updating G'DAY to model the time-course of growth and N cycling of fast-growing forest plantations, including: (1) G'DAY-Century assumed fixed C-allocation coefficients, which is clearly wrong for highly dynamic fast-growing forest plantations with seasonal growth patterns; (2) the assumption of fixed specific leaf area (SLA) and leaf N:C ratio in G'DAY-Century is no longer valid when simulating early canopy growth of young plantations; (3) to allow for moisture effects on decomposition of litter and SOM, it is necessary to take account of a soil water balance that differentiates between litter, top-soil and whole soil layers; (4) the organic matter decomposition submodel of G'DAY-Century does not fit *E. globulus* litter decomposition data (Corbeels et al., 2005b).

2. Model description

The overall structure of G'DAY is shown in Fig. 1. The model consists of four submodels: (1) plant production; (2) soil water balance; (3) decomposition; (4) soil inorganic N balance. In this section, we describe the structure and major equations of G'DAY for C and N cycling in fast-growing forest plantations. Symbols used and their units are defined in Table A.1 (Appendix A).

2.1. Plant production submodel

The plant production submodel of G'DAY, which is comprehensively described in McMurtrie and Wolf (1983), McMurtrie (1991), and Medlyn et al. (2000), simulates the C and N balances of an even-aged monoculture of trees. For application to fast-growing forest plantations we modified the model as follows: (1) radiation interception is evaluated for partially closed canopies (following Jackson and Palmer, 1981); (2) tree growth is reduced under water-limited conditions by incorporating a soil water balance submodel (see Section 2.2); (3) the maximum foliar N:C ratio of newly formed leaves depends on stand age; (4) SLA depends explicitly on foliar N:C ratio (as such it is implicitly

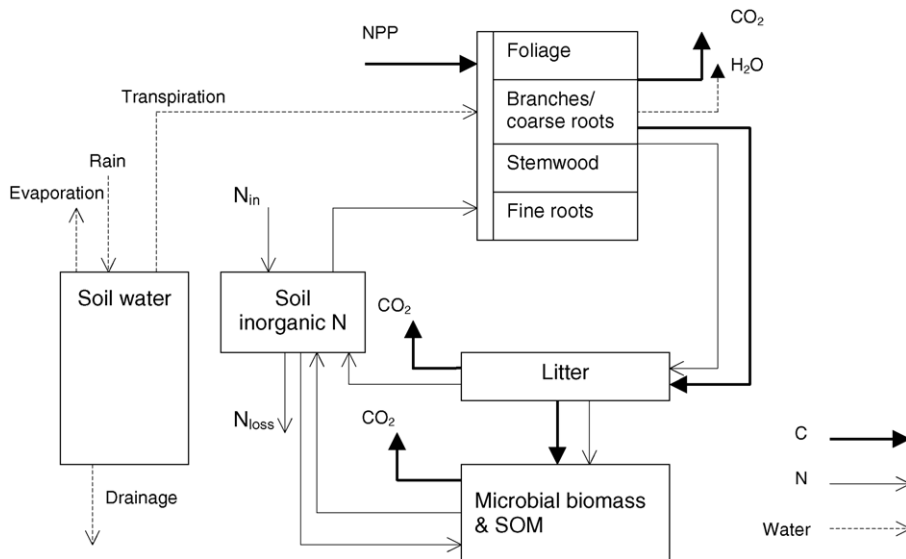


Fig. 1. The structure of G'DAY showing the key pools and fluxes of water, carbon (C) and nitrogen (N) in plant and soil. N_{in} , nitrogen input from atmospheric deposition, biological fixation and/or chemical fertiliser; N_{loss} , nitrogen loss through leaching and gaseous emissions; NPP, net primary productivity; SOM, soil organic matter.

linked to stand age); (5) C allocation to leaf, stem and branch pools is constrained by empirical allometric relationships. Here, we give only a brief outline of the plant production submodel and describe the modifications made.

The plant production submodel has five biomass pools (Fig. 1): foliage (f), branches plus coarse roots (b), stemwood (w), which is divided into sapwood (s) and heartwood (h), and fine roots (r). The branch to coarse roots ratio was set at 0.33 (Fabião et al., 1995). All pools receive C through allocation of photosynthate and N through both uptake from soil and retranslocation within the plant.

2.1.1. Net primary production (NPP)

The published G'DAY model includes a submodel that evaluates NPP from a mechanistic, biochemically based model of leaf photosynthesis (Medlyn et al., 2000). In this paper, we opted, instead, for a simpler empirical model (McMurtrie and Wolf, 1983; McMurtrie, 1991; Landsberg and Waring, 1997) which assumes that NPP is proportional to photosynthetically active radiation (PAR) absorbed by the canopy denoted by I_a , assuming that 50% of total solar radiation is PAR:

$$P_n = \varepsilon_o c_{dm} I_a f_N f_W, \quad (1)$$

where P_n ($\text{kg C m}^{-2} \text{yr}^{-1}$) is NPP, ε_o (kg DM MJ^{-1} PAR) the potential PAR utilisation efficiency, c_{dm} the conversion factor from dry matter (DM) to C, and f_N and f_W represent growth reduction factors to account for limitations by N and water, respectively. The value of ε_o is net of all growth and autotrophic respiration under the assumption that plant respiration is a fixed proportion of gross primary production (see Waring et al., 1998; Dewar et al., 1998, 1999; Medlyn et al., 2000). It is assumed that the growth reduction factors f_N and f_W range from 0 to 1, and act multiplicatively without interaction.

In this study, where G'DAY is applied to young, developing forest plantations, we evaluate radiation absorption by canopies that are partially closed (Jackson and Palmer, 1981). Therefore, PAR absorbed by the canopy (I_a) is determined as:

$$I_a = I_o \left[1 - \exp \left(-k_p \frac{L}{G_c} \right) \right] G_c, \quad (2)$$

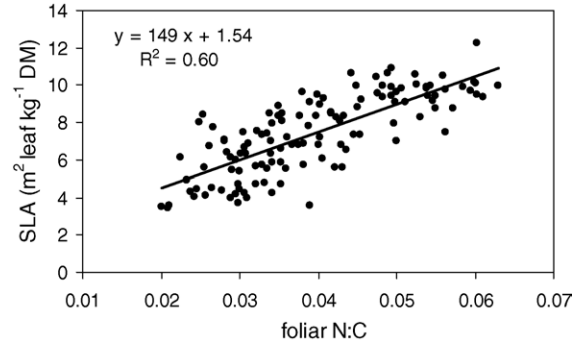


Fig. 2. Specific leaf area (SLA) of new leaves as function of foliar N:C ratio. Data from two *E. globulus* stands, respectively, at Manjimup (lat. 34°20'S, long. 116°00'E, 1023 mm rainfall), and Busselton (lat. 33°45'S, long. 115°07'E, 825 mm rainfall) in south-western Australia (T. Grove, unpublished data).

where I_o is PAR incident on the canopy, k_p the extinction coefficient for absorption of PAR by the canopy, L projected leaf area index (LAI, $\text{m}^2 \text{m}^{-2}$ ground) and G_c is fractional ground cover, which is evaluated as the ratio of L to L_{cc} , the LAI at canopy closure:

$$G_c = \frac{L}{L_{cc}}, \quad \text{if } L < L_{cc} \quad (3a)$$

$$G_c = 1, \quad \text{if } L \geq L_{cc}. \quad (3b)$$

Leaf area index (L) is related to foliar biomass (C_f , kg C m^{-2}):

$$L = \sigma \frac{C_f}{c_{dm}}, \quad (4)$$

where σ ($\text{m}^2 \text{kg}^{-1} \text{DM}$) represents specific leaf area SLA. Since simulated NPP is highly sensitive to LAI during early canopy growth, it was necessary to take into account the variation in SLA with leaf and tree age (see Sands and Landsberg, 2002). This was done in G'DAY by assuming that SLA of newly formed foliage (σ_0) is linearly related to foliar N:C ratio (n_f), which is based on data from two *E. globulus* stands in south-western Australia (Fig. 2):

$$\sigma_0 = \sigma_i + \frac{n_f}{n_{fY \max}} (\sigma_{\max} - \sigma_i), \quad (5)$$

with $n_f \leq n_{fY \max}$,

where σ_{\max} is the maximum SLA of new leaves, which is achieved when n_f is equal to the maximum N:C ratio observed in foliage of young trees, $n_{fY \max}$, and σ_i is

the y-intercept in the relationship between σ_0 and n_f (Fig. 2). In G'DAY, LAI is a dynamic variable that is predicted from the difference between LAI of new leaf production (with SLA of σ_0) and LAI of senescing leaves (obtained by multiplying current LAI by leaf turnover rate l_f that is estimated from Eq. (17)).

The reduction in NPP due to N limitation (f_N) depends linearly on foliar N:C ratio (n_f) if n_f is less than a critical value ($n_{f\text{crit}}$):

$$f_N = \frac{n_f}{n_{f\text{crit}}}, \quad \text{if } n_f < n_{f\text{crit}} \quad (6a)$$

$$f_N = 1, \quad \text{if } n_f \geq n_{f\text{crit}}. \quad (6b)$$

Thus, it is assumed that there is a critical foliar N concentration, below which photosynthesis is N-limited (see McMurtrie, 1991, for a detailed discussion). The value of $n_{f\text{crit}}$ decreases over time. It is proportional to the maximum leaf N:C ratio ($n_{f\text{max}}$), which is a function of stand age (t):

$$n_{f\text{crit}} = a_N n_{f\text{max}}, \quad (7)$$

where a_N is a constant, and

$$n_{f\text{max}} = n_{fY\text{max}} - (n_{fY\text{max}} - n_{fM\text{max}}) \left(\frac{t}{T_M} \right), \quad (8a)$$

if $t < T_M$

$$n_{f\text{max}} = n_{fM\text{max}}, \quad \text{if } t \geq T_M. \quad (8b)$$

Thus, $n_{fY\text{max}}$ is the maximum N:C ratio of newly formed leaves at stand age $t=0$, and $n_{fM\text{max}}$ is the maximum N:C ratio of newly formed leaves in a mature stand of age $t=T_M$ or older.

The model calculates a stand water balance (see below; Section 2.2). Both NPP and decomposition are reduced if plant available soil water is low. The effects of soil water content of top-soil and forest floor on decomposition is described in Corbeels et al. (2005b).

The water limitation factor f_W for NPP depends on total plant available water (W_t , mm) to a specified soil depth as follows:

$$f_W = \frac{W_t/W_{t\text{max}}}{FP_{w\text{crit}}}, \quad \text{if } \frac{W_t}{W_{t\text{max}}} < FP_{w\text{crit}} \quad (9a)$$

$$f_W = 1, \quad \text{if } \frac{W_t}{W_{t\text{max}}} \geq FP_{w\text{crit}}, \quad (9b)$$

where $W_{t\text{max}}$ is maximum plant available water PAW and $FP_{w\text{crit}}$ is an empirical parameter representing the fractional PAW, below which production is proportional to PAW. The relationship of f_W to the ratio $W_t:W_{t\text{max}}$ is functionally analogous to equations used in other models for the ratio of actual to potential evapotranspiration (e.g. Slabbers, 1980; Dunin, 2002).

2.1.2. Carbon allocation

Carbon allocation is highly variable during the early development of forest plantations. Allocation to foliage usually decreases with stand age whereas allocation to stemwood increases (e.g. Mäkelä and Hari, 1986; Cannell and Dewar, 1994; Magnani et al., 2000). Environmental conditions also affect patterns of allocation in trees. For example, the proportion of NPP that is allocated to fine roots is generally higher on sites that experience soil water and/or nutrient stresses (e.g. Santantonio, 1989; Keith et al., 1997).

Previous versions of G'DAY have assumed constant C-allocation coefficients, or allocation coefficients that are functions of leaf N:C ratio. In this version, we employ the following empirical model for C allocation as a function of tree height. Leaf versus stem allocation is constrained by an empirical equation for the ratio (LS, dimensionless) of projected leaf area index (L) to stem sapwood cross-sectional area (A_s , $\text{m}^2 \text{m}^{-2}$ ground) (Medhurst et al., 1999). In most species this ratio declines with increasing height (e.g. Medhurst et al., 1999; Magnani et al., 2000). We assume that the ratio varies from LS_0 to LS_1 as a linear function of tree height (H , m):

$$LS = LS_0, \quad \text{if } H \leq H_0 \quad (10a)$$

$$LS = LS_0 + \frac{(LS_1 - LS_0)(H - H_0)}{H_1 - H_0}, \quad (10b)$$

if $H_0 < H < H_1$

$$LS = LS_1, \quad \text{if } H \geq H_1. \quad (10c)$$

Average tree height is calculated from stemwood mass (C_w , kg C m^{-2}) using an empirical allometric relationship:

$$H = b_1 C_w^{b_2}, \quad (11)$$

where b_1 and b_2 are constants.

Sapwood cross-sectional area is calculated from sapwood mass (C_s , kg C m⁻²), the height and sapwood density (ρ , kg DM m⁻³):

$$A_s = \frac{C_s}{\rho H}, \quad (12)$$

where C_s is estimated from Eqs. (18a)–(18c).

There are several ways that the constraint (Eqs. (10a)–(10c)) could be incorporated into G'DAY, e.g. through controls on leaf versus stem allocation as in the 3-PG model (Sands and Landsberg, 2002) or controls on leaf and sapwood turnover. Our approach involves assuming Eqs. (10a)–(10c) represents a target leaf:sapwood area ratio that is approached by varying leaf and stem-allocation coefficients. Leaf allocation depends on the value of L/A_s relative to the target value LS, declining from a maximum value $a_{f\max}$ to zero with increasing L/A_s . The variation of a_f is characterised by a parameter δ_{LS} :

$$a_f = a_{f\max}, \quad \text{if } \frac{L}{A_s} \leq LS(1 - \delta_{LS}) \quad (13a)$$

$$a_f = 0.5 a_{f\max} \left(1 + \frac{(1 - (L/A_s)/LS)}{\delta_{LS}} \right),$$

$$\text{if } LS(1 - \delta_{LS}) < \frac{L}{A_s} < LS(1 + \delta_{LS}) \quad (13b)$$

$$a_f = 0, \quad \text{if } \frac{L}{A_s} \geq LS(1 + \delta_{LS}) \quad (13c)$$

Eqs. (13a)–(13c) is a goal-seeking formulation of the process of leaf versus stem allocation (cf. Thornley and Johnson, 1990), where the goal is the relationship (Eqs. (10a)–(10c)), which expresses leaf:sapwood area ratio as a function of tree height. If simulated leaf:sapwood area ratio is below (or above) the target value LS, allocation to leaves a_f increases (or decreases) relative to stem allocation a_s . However, the value of a_f cannot exceed $a_{f\max}$. The parameter δ_{LS} characterises how a_f and a_s respond when the leaf:sapwood area ratio departs from the target value LS. If $\delta_{LS} \ll 1$, then the simulated leaf:sapwood area ratio will closely track the target value LS. However, as δ_{LS} increases, the allocation coefficients are less responsive, and leaf:sapwood area ratio tracks the target LS less tightly.

Branch allocation is constrained in a similar way by an empirical allometric relationship between branch

(C_b , kg C m⁻²) and stemwood mass (C_w , kg C m⁻²):

$$C_b = b_3 C_w^{b_4}, \quad (14)$$

where b_3 and b_4 are constants. This constraint is imposed through a goal-seeking formulation of the process of branch versus stem allocation, analogous to Eqs. (13a)–(13c). The goal is the branch–stem allometric relationship (Eq. (14)):

$$a_b = a_{b\max}, \quad \text{if } C_b \leq b_3 C_w^{b_4} (1 - \delta_{BS}) \quad (15a)$$

$$a_b = 0.5 a_{b\max} \left(1 + \frac{(1 - (C_b)/(b_3 C_w^{b_4}))}{\delta_{BS}} \right),$$

$$\text{if } b_3 C_w^{b_4} (1 - \delta_{BS}) < C_b < b_3 C_w^{b_4} (1 + \delta_{BS}) \quad (15b)$$

$$a_b = 0, \quad \text{if } C_b \geq b_3 C_w^{b_4} (1 + \delta_{BS}), \quad (15c)$$

where the parameter δ_{BS} characterises the variability in a_b . If simulated branch mass is below (or above) the target value calculated from Eq. (14), then allocation to branches a_b increases (or decreases) relative to stem allocation a_s . However, the value of a_b cannot exceed $a_{b\max}$. The parameter δ_{BS} characterises how a_b and a_s respond when the branch mass departs from the target value C_b . If $\delta_{BS} \ll 1$, then the simulated branch mass will closely track the target value C_b . However, as δ_{LS} increases, the allocation coefficients are less responsive, and branch mass tracks the target less tightly.

The allocation coefficient to fine roots a_r is held constant for a given site, while stem allocation is calculated as the residual:

$$a_s = 1 - a_f - a_b - a_r. \quad (16)$$

According to the allocation model (Eqs. (13a)–(13c), (15a)–(15c) and (16)), a shift in either leaf or branch allocation is matched by an opposing shift in stem allocation. It is acknowledged that the above allocation model does not explain the physiological processes governing allocation of assimilates. Though mechanisms underlying the relationship (Eqs. (10a)–(10c)) have been parameterised for some forest systems (e.g. Dewar, 1993; Magnani et al., 2000), there is considerable doubt about how parameters change with tree size and age. We adopt the above empirical approach because our primary aim is to develop a tree growth

model that works across a range of environmental conditions, and can be used for predicting associated N cycling in the plant–soil system.

2.1.3. Litter production

We assume that litter production from each tree biomass pool is proportional to its pool size, thus implying a specific litterfall rate for each pool. Because field measurements (F.J. Hingston, unpublished data) indicate higher leaf litterfall during dry spells, we made leaf litterfall rate dependent on soil water content by incorporating an empirical rate modifier:

$$l_f = l_{f \max}, \quad \text{if } \frac{W_t}{W_{t \max}} \leq \text{FL}_{w \min} \quad (17a)$$

$$l_f = l_{f \max} - (l_{f \max} - l_{f \min}) \left(\frac{W_t / W_{t \max} - \text{FL}_{w \min}}{\text{FL}_{w \max} - \text{FL}_{w \min}} \right),$$

$$\text{if } \text{FL}_{w \min} < \frac{W_t}{W_{t \max}} < \text{FL}_{w \max} \quad (17b)$$

$$l_f = l_{f \min}, \quad \text{if } \frac{W_t}{W_{t \max}} \geq \text{FL}_{w \max}, \quad (17c)$$

where $l_{f \max}$ (yr^{-1}) is the maximum specific leaf litterfall rate occurring when fractional plant available water ($W_t:W_{t \max}$) is below a critical minimum value ($\text{FL}_{w \min}$) and $l_{f \min}$ is the minimum specific leaf litterfall rate occurring when fractional plant available water is above a critical maximum value ($\text{FL}_{w \max}$). Due to a lack of detailed data, we assumed fixed specific turnover rates for the other tree biomass pools, including conversion of sapwood into heartwood; the same values were applied to all three eucalypt stands (see Section 4).

Thus, the daily increment in C content of biomass ΔC_i is calculated from the following difference equations (McMurtrie, 1991):

$$\Delta C_i = a_i P_n - l_i C_i \quad (18a)$$

$$\Delta C_s = a_s P_n - l_s C_s - r_s C_s \quad (18b)$$

$$\Delta C_h = r_s C_s - l_h C_h, \quad (18c)$$

where C_i is the C content of tree biomass pool i ($i = b, f, r$), a_i the allocation coefficient to tree biomass pool i , l_i the litter production rate of the i th tree biomass pool

and r_s is the turnover rate of sapwood to heartwood. Stemwood mass is $C_w = C_s + C_h$.

2.1.4. Nitrogen allocation

Nitrogen allocation to new tree growth is derived from N uptake by trees from the soil inorganic N pool plus N retranslocated from senesced plant tissues. Nitrogen allocation within the plant is based on C allocation and the assumption that the N:C ratios of newly formed branch and sapwood are constant, whereas the N:C ratios of newly formed leaves and fine roots vary within limits depending on the amount of N available for allocation. For leaves, maximum N:C ratio ($n_{f \max}$) is age-dependent, declining at a constant rate from $n_{fY \max}$ in young trees of age zero to a minimum value of $n_{fM \max}$ in a mature stand of age $t = T_M$ (Eq. (8)). For roots, maximum N:C ratio ($n_{r \max}$) is constant.

Wood N is further divided into structural and non-structural components (Medlyn et al., 2000). For each tree biomass pool, except structural wood N, we assume that prior to litter production a fixed fraction of N is retranslocated to a labile plant N pool, which is available for immediate retranslocation to new growth. We also assume a fixed rate of retranslocation from the non-structural N wood component to the labile N pool.

2.2. Forest floor and soil water balance

A simple water balance model that calculates water storage in both the forest floor and soil root zone was incorporated into the new version of G'DAY. The model has the provision for three layers: forest floor (ff), top-soil (top) and sub-soil (sub). It is important to simulate the water content of the forest floor and the top-soil (e.g. 0–20 cm) layer because N mineralisation occurs mainly in the top-soil (e.g. Connell et al., 1995) where moisture content is most variable.

The daily increment in PAW (ΔW , mm) for the three layers is calculated as:

$$\Delta W_{\text{ff}} = R_{\text{eff}} - E_{\text{ff}} - D_{\text{ff}} \quad (19a)$$

$$\Delta W_{\text{top}} = D_{\text{ff}} - E_{\text{top}} - T_{\text{top}} - D_{\text{top}} \quad (19b)$$

$$\Delta W_{\text{sub}} = D_{\text{top}} - T_{\text{sub}} - D_{\text{sub}}, \quad (19c)$$

where the subscripts, ff, top and sub refer, respectively, to the forest floor, top-soil and sub-soil layers, R_{eff} is daily effective rainfall (after subtracting water loss

from canopy interception, [McMurtrie et al., 1990](#)), E_{ff} and E_{top} are daily evaporation from the forest floor and the top-soil layer, and D and T represent daily rates of drainage and tree water use from each layer with:

$$T_{\text{top}} = \min(q_{\text{et}} T_t, W_{\text{top}}) \quad (20a)$$

$$T_{\text{sub}} = \min(T_t, W_t) - T_{\text{top}}, \quad (20b)$$

where q_{et} is an empirical constant representing the fraction of water uptake from top-soil when both soil layers are at field capacity and the subscript t refers to the ‘total’ over the two soil layers.

Daily total transpiration by the tree canopy (T_t) is calculated using the Penman–Monteith equation as described by [McMurtrie et al. \(1990\)](#), with a modification to evaluate diurnal integrals of transpiration. Canopy conductance is estimated from LAI and maximum stomatal conductance modified by minimum temperature and by PAW ([McMurtrie et al., 1990](#)). The effect of PAW on conductance is characterised by parameters $FT_{\text{w min}}$ and $FT_{\text{w max}}$ ([Table 2](#)) that represent, respectively, the soil water content below which conductance is zero and above which there is no effect of soil water on conductance ([Table 2](#), see also [Hingston et al., 1998](#) for more details).

Daily effective rainfall (R_{eff}) enters the forest floor. If the water content of this layer exceeds its water holding capacity, the excess water (D_{ff}) is transferred to the top-soil layer. Similarly, water in excess of the water holding capacity of the top-soil layer (D_{top}) is drained to the sub-soil layer. Overall, drainage losses out of the soil profile (D_{sub}) occur when the water content of the sub-soil layer exceeds its water holding capacity.

In addition to evaporation of rainfall intercepted by the canopy, evaporation occurs also from the forest floor (E_{ff}) and the top-soil layer (E_{top}). Following [Ritchie \(1972\)](#), we assume that evaporation occurs in two stages: the constant and the falling rate. In the constant stage, when the water content of the forest floor or top-soil layer is above a threshold value, evaporation is limited only by the supply of energy. Evaporation then takes place at the potential evaporation rate (E_o), calculated from the Penman equation with net radiation corrected for canopy shading:

$$E_o = \frac{1}{\lambda} \left[\frac{s}{s + \gamma} \right] R_n \exp(-k_t L), \quad (21)$$

where λ is the latent heat of vaporisation, s the slope of the saturation vapour pressure–temperature curve, γ the psychrometric constant, R_n net radiation, k_t the extinction coefficient for absorption of total net radiation by canopy and L is one-sided LAI.

Once the water content has decreased below a threshold value, evaporation is controlled by hydraulic properties and declines rapidly with decreasing water content. This is the ‘falling rate’ stage and evaporation is reduced by a factor proportional to the relative moisture content of the layer:

$$E_{\text{ff}} = b_{\text{ff}} E_o \quad (22a)$$

$$E_{\text{top}} = b_{\text{top}} (E_o - E_{\text{ff}}), \quad (22b)$$

where b_{ff} and b_{top} are functions representing effects of reduced moisture content on evaporation from the litter and top-soil layer that are analogous to [Eqs. \(9a\) and \(9b\)](#).

2.3. Decomposition model

The new decomposition submodel used in this version of G'DAY is fully described in [Corbeels et al. \(2005b\)](#), where it is tested against mass and N loss measured in decomposing *E. globulus* litter. It replaces the CENTURY-based decomposition submodel in the original version of G'DAY ([Comins and McMurtrie, 1993](#)) because the CENTURY-based submodel failed to simulate N mineralisation-immobilisation dynamics in decomposing eucalypt leaf material. The new model uses a more mechanistic approach to describe N mineralisation-immobilisation turnover and the interactions between C and N dynamics in decomposing litter and SOM. The submodel includes above- and below-ground litter pools and three SOM pools (microbial biomass, *Young* and *Old* SOM) with different turnover times. Rates of decomposition are modified by temperature, moisture, lignin content and N availability. Stabilisation of SOM is simulated by transferring fractions of decomposed microbial biomass and *Young* SOM into more recalcitrant pools (respectively into *Young* and *Old* SOM). Nitrogen is mineralised to, or immobilised from, the soil inorganic N pool to maintain the N:C ratio of decomposing microbial biomass within a specified range. Balancing potential microbial N demand against inorganic N availability determines whether the activity of decomposers is limited by N. If

so, then simulated decomposition fluxes are reduced. The maximum rate of microbial N uptake is proportional to soil inorganic N content. Lignin transformation to *Young* SOM promotes additional N immobilisation into the *Young* SOM pool, which simulates the process of chemical N immobilisation.

2.4. Soil inorganic nitrogen balance

The daily increment of the soil inorganic N pool (ΔN_{inorg} , kg N m⁻²) in G'DAY is calculated from the difference between the following influxes and effluxes:

$$\Delta N_{\text{inorg}} = N_{\text{min}} - N_{\text{imm}} - A_{\text{imm}} + N_{\text{in}} - N_{\text{loss}} - U_{\text{p}}, \quad (23)$$

where N_{min} is the rate of gross N mineralisation, N_{imm} the rate of gross N immobilisation through microbial uptake, A_{imm} the rate of abiotic or chemical N immobilisation into *Young* SOM associated with decomposition of lignin, N_{in} the rate of external input from atmospheric deposition, fertiliser and/or biological N fixation, N_{loss} the rate of N losses through leaching and/or gaseous emission, and U_{p} is the rate of N uptake by plants. N_{min} , N_{imm} and A_{imm} are calculated in the decomposition submodel, using equations given in Corbeels et al. (2005b).

In G'DAY we assume that the rate of overall N loss (N_{loss}) from the soil–plant system is proportional to the inorganic N pool:

$$N_{\text{loss}} = \lambda_1 N_{\text{inorg}}, \quad (24)$$

where λ_1 (yr⁻¹) is a site-specific empirical rate constant for both gaseous and leaching losses (McMurtrie et al., 2001). The potential for N losses under forest plantations depends on a number of factors, including soil type, rainfall and rooting depth, and is likely to vary with stand age (Aronsson et al., 2000; Laclau et al., 2003). For simplicity, we hold λ_1 constant over the whole year. However, we acknowledge that this is probably a gross simplification for many forest plantation systems.

Similarly, N uptake by trees is also assumed to be proportional to soil inorganic N:

$$U_{\text{p}} = \lambda_{\text{p}} N_{\text{inorg}}, \quad (25)$$

where λ_{p} (yr⁻¹) is an empirical rate constant, representing the potential availability of soil inorganic N to

plants (McMurtrie et al., 2001). An upper limit to N uptake is imposed by assuming that plant N:C ratios cannot exceed maximum values (see Eq. (8)). If N uptake is less than N demand by trees to meet minimum N:C ratios, NPP is reduced. This formulation of plant N uptake is analogous to our equation for microbial N uptake (Eq. (9) in Corbeels et al., 2005b).

3. The experiments and dataset

We parameterised and tested G'DAY for *E. globulus*, using experimental data from three stands in south-western Australia. This region has a Mediterranean climate with hot, dry summers and cool, wet winters, with the majority of rainfall occurring in the months May to September. The three stands (1) Mumballup (33°33'S, 116°4'E, 950 mm rainfall yr⁻¹), (2) Darkan (33°19'S, 116°35'E, 600 mm rainfall yr⁻¹), and (3) Northcliffe (34°41'S, 116°11'E, 1500 mm rainfall yr⁻¹), have been monitored with regular measurements of tree growth and N mineralisation (Hingston and Galbraith, 1998; O'Connell and Rance, 1999). Before planting of *E. globulus*, all sites had been under conventional, legume-based farming with annual chemical fertiliser addition. Selected characteristics of the three sites are listed in Table 1. At the Mumballup site, the soil is a shallow Xanthic Ferralsol (FAO classification) with a surface sandy loam horizon. Tree roots penetrate to the undulating basement rock at a depth of 1.5–1.7 m (Hingston et al., 1998). *E. globulus* was planted in 1988 at a stocking of 1250 stems ha⁻¹. The Darkan site has a yellow mottled duplex soil (Dystric Planosol) that comprises a sandy loam surface horizon over a sandy clay sub-soil. Root penetration at the site was restricted by a very hard and compacted horizon at about 3 m depth. *E. globulus* was first planted here in 1987 with a stocking of 680 stems ha⁻¹. The plantation at the Northcliffe site was established in 1986 (1250 stems ha⁻¹) on a gravelly Ferric Lixisol with a surface sandy loam horizon, without any obvious constraint for root penetration.

Daily meteorological data on precipitation, minimum and maximum air temperature, and total radiation have been recorded by automatic weather stations at each site from 1991 to 1994. For other years, we used data generated from interpolation of daily data recorded at nearby stations (for details, see SILO Data Drill; <http://www.dnr.qld.gov.au/silo>). Soil water con-

Table 1
Selected site characteristics for the three *E. globulus* stands

Site	Mean annual rainfall (mm)	Clay + silt ^a (g kg ⁻¹)	Rooting depth (m)	WHC ^b (mm)	Organic C ^a (g kg ⁻¹)	Total N ^a (g kg ⁻¹)	Labile N ^{a,c} (% of total N)
Mumballup	959	140	1.7	250	44.4	2.01	1.1
Darkan	590	110	3.0	227	27.4	0.90	1.7
Northcliffe	1450	40	>6.0	>500	37.0	1.87	1.0

^a In top-soil (0–20 cm).

^b Soil water holding capacity.

^c NH₄-N released during 7-day anaerobic incubation at 40 °C.

tent, stem diameter (at 1.3 m over bark) and height of trees, LAI and leaf litterfall were recorded monthly at each site between 1990 and 1993. Soil water content was measured with a neutron moisture gauge (DIDCOT Instruments, Oxford, UK) to depths of 3 m. LAI was estimated using the LAI-2000 plant canopy analyser (LI-COR, Lincoln, NE, USA) (Hingston et al., 1998). Stem dry weight (wood plus bark dry matter ha⁻¹) was estimated from the stocking rate, and monthly measurements of tree height and stem diameter using an allometric relationship, previously developed by Hingston and Galbraith (1998) from sampling trees at the three sites above and three other *E. globulus* stands in south-western Australia. Leaf litter production was estimated from litter collections over monthly time intervals.

Nitrogen mineralisation was measured in the top 20 cm soil layer at 4 weekly intervals over a period of 2.8 years (Mumballup, start of measurements in March 1992) and 3 years (Darkan and Northcliffe, starting in January 1992) using the in situ coring technique; experimental details and results of these measurements are fully described in O'Connell and Rance (1999).

4. Model parameterisation and results

In this section we explain how G'DAY was parameterised for the three *E. globulus* stands. The general procedure was to use a common set of model parameters for all three sites with best available empirical values or standard default values. Parameterisation involved several steps including: (1) comparison of simulated with measured soil water content to parameterise the soil water balance submodel; (2) estimation of parameters controlling leaf litterfall to fit observed leaf litterfall data; (3) parameterisation of the plant production and C-allocation submodel to fit stem biomass and LAI

data; (4) initialisation of the soil C and N pools for each site based on soil N mineralisation data from laboratory incubations.

To evaluate the accuracy of the model simulations, the root mean square error (RMSE), linear correlation coefficient (r), relative model efficiency (EF) and relative error (E) were calculated for each set of simulated and observed values of plant available soil water, leaf litter production, LAI, stem biomass and soil N mineralisation. Model efficiency, EF, is defined as: $EF = 1 - \left(\frac{\sum_{i=1}^n (O_i - P_i)^2}{\sum_{i=1}^n (O_i - \bar{O})^2} \right)$, where O_i are the observed values, P_i the predicted values, \bar{O} the mean of the observed data, and n is the number of paired values (Loague and Green, 1991). The model efficiency provides a comparison of the efficiency of the model to the efficiency of describing the data as the mean of the observations. Values of EF may be positive or negative with a maximum value of 1. A positive value indicates that the simulated values describe the trend in the measured data better than the mean of the observations. A negative value indicates that the simulated values describe the data less well than a mean of the observations. The relative error, E , determines the bias in the total difference between simulations and measurements and is defined as: $E = (100/n) \sum_{i=1}^n (O_i - P_i) / O_i$ (Addiscott and Whitmore, 1987).

Note, however, that r and EF are of limited use in determining accuracy of model simulations for cases where there is no clear trend in the measured data to give a spread of paired observed and predicted values.

Parameter values for the water balance, plant production and soil inorganic N balance submodels are given in Table 2. The decomposition submodel was parameterised previously by simulating mineralisation from *E. globulus* foliar and woody residues (see Corbeels et al., 2005b). For each model parameter

Table 2

Parameter values in the water balance, plant production and soil N balance submodels estimated for *E. globulus* plantations in south-western Australia

Parameter	Value	Site- or species-specific	Source
$a_{b \max}, a_{f \max}$	0.40, 0.33	Species	Fitted
a_r	0.42 (Mumballup), 0.49 (Darkan), 0.36 (Northcliffe)	Both	Fitted
a_N	0.75	Species	Based on Pereira et al. (1992)
b_1, b_2	4.83, 0.350	Species	Based on F.J. Hingston, unpublished data
b_3, b_4	5.61, 0.346	Species	Based on F.J. Hingston, unpublished data
c_{dm}	0.48 g C g ⁻¹ DM	Species	Nominal value
$FP_{w \text{ crit}}$	0.6	Species	Beadle et al. (1995)
$FL_{w \text{ max}}$	0.6	Both	Fitted
$FL_{w \text{ min}}$	0.0	Both	Based on F.J. Hingston, unpublished data
$FT_{w \text{ max}}$	0.4	Species	Fitted
$FT_{w \text{ min}}$	0.028	Species	Fitted
H_0, H_1	5, 30	Species	Based on F.J. Hingston, unpublished data
k_p	0.5	Species	Linder (1985)
k_t	0.4	Species	Ritchie (1972)
l_b, l_r, l_s, l_h	0.03, 2.4, 0, 0 yr ⁻¹	Species	F.J. Hingston, unpublished data, Kätterer et al. (1995)
L_{cc}	2.0 m ² m ⁻²	Species	Fitted
$l_{f \max}$	0.6 (Mumballup, Darkan), 0.8 (Northcliffe) yr ⁻¹	Both	Fitted
$l_{f \min}$	0.2 (all sites) yr ⁻¹	Both	Fitted
LS_0, LS_1	8000, 2700	Species	F.J. Hingston, unpublished data
L_{vap}	2.45×10^{-6} J kg ⁻¹ (20 °C)	–	Physical constant
n_b, n_{nw}, n_{sw}	0.0035, 0.0025, 0.0015	–	A.M. O'Connell, unpublished data
$n_{fM \max}$	0.022 (see Fig. 7)	Species	Cromer and Williams (1982), Judd et al. (1996), Bennett et al. (1997), A.M. O'Connell, unpublished data
$n_{f \max 0}$	See Fig. 7, Eq. (11)	Species	Cromer and Williams (1982), Judd et al. (1996), Bennett et al. (1997), A.M. O'Connell, unpublished data
$n_f Y_{\max}$	0.066 (see Fig. 7)	Species	Cromer and Williams (1982), Judd et al. (1996), Bennett et al. (1997), A.M. O'Connell unpublished data
$n_r \max$	0.017	Species	Bauhus et al. (2000)
r_s	0.1 yr ⁻¹	Species	Based on S.J. Rance, unpublished data
t_b, t_f, t_r	0.5, 0.45, 0.	Species	F.J. Hingston, unpublished data, Gordon and Jackson (2000)
T_M	6 yr (see Fig. 7)	Species	Cromer and Williams (1982), Judd et al. (1996), Bennett et al. (1997), A.M. O'Connell, unpublished data
q_{et}	0.7	Both	Fitted
$W_{ff \max}$	8 mm (all sites)	Site	Estimated
$W_{t \max}$	250 mm (Mumballup), 230 mm (Darkan), 600 mm (Northcliffe)	Site	Based on data from Hingston et al. (1998)
$W_{top \max}$	50 mm (all sites)	Site	Based on F.J. Hingston, unpublished data
γ	66 Pa °C ⁻¹	–	Physical constant
δ_{BS}	0.5	Species	Fitted
δ_{LS}	0.5	Species	Fitted
ϵ_o	3.3×10^{-3} kg DM MJ ⁻¹ PAR	Species	Sands and Landsberg (2002)
λ_l	0 yr ⁻¹	Both	Based on Carlyle (1995)
λ_p	10.2 yr ⁻¹	Species	Fitted
ρ	480 kg DM m ⁻³ .	Species	S.J. Rance, unpublished data
σ_{\max}	11 m ² kg ⁻¹ DM (see Fig. 2)	Species	T. Grove, unpublished data

Abbreviations: C, carbon; DM, dry matter; PAR, photosynthetically active radiation.

we have indicated in Table 2 whether the value was obtained directly from measurements at the sites, was an independent empirical value from the literature or was estimated by fitting G'DAY to observed data.

4.1. Soil water balance

The first step was to parameterise the water balance submodel using information on maximum available soil water in the root zone ($W_{t\max}$, Table 2), daily weather data, and observed LAI data. The model was first calibrated to soil water data at the Mumballup site by adjusting the critical soil water contents, $FT_{w\min}$ and $FT_{w\max}$, that characterise the water dependence of stomatal conductance (Table 2, see also Hingston et al., 1998 for more details). All other parameters in the water balance submodel were given values a priori on the basis of published information (see Table 2). The soil moisture profile shows high rates of recharge in autumn and drying during late spring (Fig. 3a). The model's ability to predict rates of drying and rewetting is crucial because simulated NPP is dependent upon soil water content if $W_t < 0.6 W_{t\max}$ (see below, i.e. if root-zone PAW is less than 150 mm at Mumballup, Eq. (9)).

The parameterised water balance submodel was then applied to the other 2 sites, each time with maximum available soil water content in the root zone, daily weather data and observed LAI values as site-specific input. This provides an independent test of the model. The results for the Darkan site (Fig. 3b) show a strong correlation between observed and simulated values ($r = 0.95$) with high model efficiency ($EF = 0.89$) and low bias ($E = -9$), illustrating that the simple water balance submodel of G'DAY was able to provide a good simulation of soil water dynamics under eucalypt stands in the sandy soils of south-western Australia. Trees at Northcliffe were able to extract water at depths up to 6 m or more ($W_{t\max} = 600$ mm, Table 2, Hingston et al., 1998), so available soil moisture measurements to depths of 3 m (not shown) do not reflect water that is accessible by trees on this site.

4.2. Litter production parameters

Observations at the three sites showed that leaf litterfall rates varied throughout the year, with in general higher rates during the dry season when soil

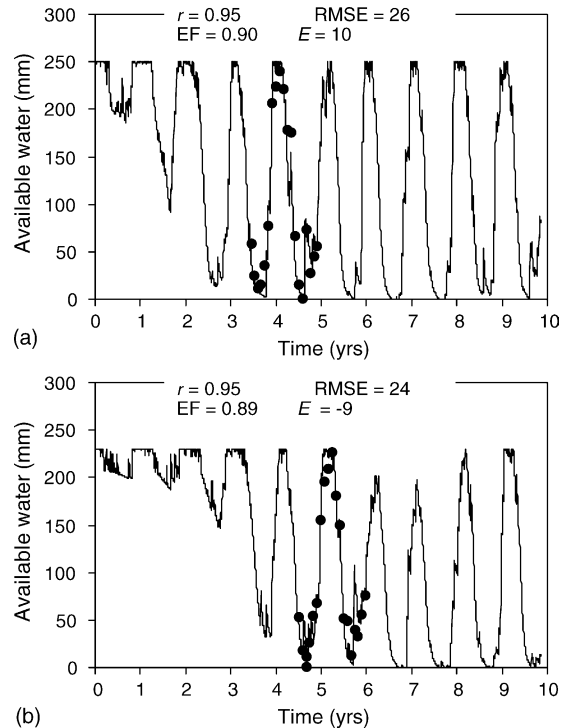


Fig. 3. Comparison of measured (symbols) and simulated (line) plant available water (mm) in the root-zone (to 3 m soil depth) under *E. globulus* plantations at (a) Mumballup and (b) Darkan. Simulations commenced with trees planted on 1st July 1988 and 1st July 1987 at Mumballup and Darkan, respectively. Measured data are from Hingston et al. (1998). Simulations were obtained by parameterising the water balance model of G'DAY to the Mumballup site, and applying the calibrated model to the Darkan site. r , coefficient of linear correlation between observed and simulated values; RMSE, root mean square error; EF, relative model efficiency; E , relative error.

water content was low. Therefore, for each site, we assumed that the specific rate of leaf litterfall increased from a minimum value ($l_{f\min}$) when the soil is wet ($W_t: W_{t\max} \geq FL_{w\max}$) to a maximum ($l_{f\max}$), when the soil is dry ($W_t = 0$) (Eq. (17), Table 2). Parameter values for $l_{f\min}$, $l_{f\max}$ and $FL_{w\max}$ at each site were then estimated by fitting the model (using the above simulated water balance) to leaf litterfall data with LAI adjusted to match observations. Results of these simulations are presented in Fig. 4, together with cumulative amounts of observed and simulated leaf litterfall during the period when litterfall was measured. Fig. 4 shows that the model did not perform well in fitting the timing and magnitude of the observed peaks of leaf litterfall. This was reflected in the large measures for model error

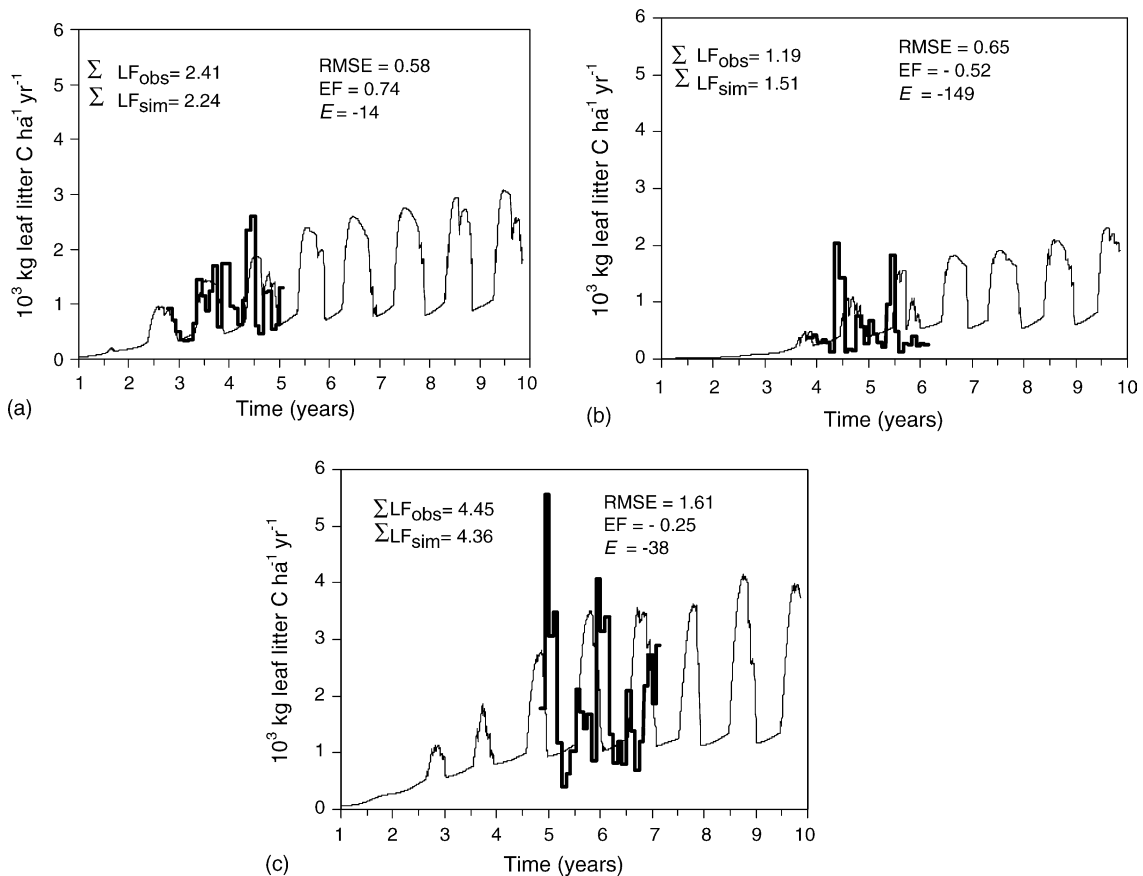


Fig. 4. Comparison of measured (bold line) and simulated (fine line) monthly leaf litter production from *E. globulus* plantations at (a) Mumballup, (b) Darkan and (c) Northcliffe. Simulations commenced 1st July 1988, 1st July 1987 and 1st July 1986 at Mumballup, Darkan and Northcliffe, respectively. Measured data are unpublished data from Hingston F.J. Simulated lines were obtained by adjusting parameter values for leaf litterfall in G'DAY (see Table 2). $\sum LF_{obs}$ and $\sum LF_{sim}$ represent, respectively, cumulative amounts of observed and simulated leaf litterfall (in Mg C ha⁻¹) during the 38-month period when litterfall was measured. RMSE, root mean square error; EF, model efficiency; *E*, relative error.

(RMSE, EF) and bias (*E*). It suggests that drought stress effects on leaf senescence are complex and that other mechanisms (such as wind, temperature, radiation and age effects) may have to be included to accurately predict leaf fall. Simulated seasonal timing of peak leaf litterfalls often mismatched observations possibly for these reasons (Fig. 4). However, despite this, simulation of the total leaf litterfall amounts that occurred during the measuring period matched measurements reasonably well.

The specific rate of branch/coarse root litter production (l_b) was assumed to be a constant 0.03 yr⁻¹ for all sites in this study. This value represents a mean calculated from all available observed data on 'non-leaf' litterfall at the three sites. 'Non-leaf' litterfall rate was

estimated at 0.028, 0.027 and 0.035 yr⁻¹, respectively at Mumballup, Darkan and Northcliffe (F. Hingston, unpublished data). Likewise, the specific rate of fine root litter production (l_r) was given a constant value of 2.4 yr⁻¹ for all three sites, based on data from Kätterer et al. (1995). Litter production from stem (l_s , l_h) was assumed to be negligible and therefore set at zero. The rate of conversion of sapwood to heartwood (r_s) was set at 0.1 yr⁻¹.

4.3. Plant production submodel

The next step was to parameterise the plant production submodel. Potential radiation-use efficiency (ϵ_0) was set at 3.3×10^{-3} kg DMMJ⁻¹ PAR, which

represents a realistic upper limit for *E. globulus* in West Australia (Sands and Landsberg, 2002), and is similar to the values estimated by McMurtrie et al. (1994). It is lower than the theoretical maximum of 3.8×10^{-3} kg DM MJ⁻¹ PAR, proposed by Landsberg et al. (2003), to account for limitations by non-optimal temperatures (Sands and Landsberg, 2002). The effective value of radiation-use efficiency in the model was obtained by modifying the potential value (ϵ_0) for water and N availability (Eq. (1)). Based on measured responses of eucalypt growth to water availability (Beadle et al., 1995), we assumed that NPP declines linearly with available soil moisture below a critical soil water content (FP_{w crit}), calculated as 60% of maximum available water in the soil profile, and reaches zero when available soil water is zero (see Eq. (9)). The critical foliar N:C ratio for maximum productivity was set at 0.05 and 0.016 ($a_N = 0.75$, Eq. (7)), respectively, for young and mature trees, corresponding to approximately 2 g N m⁻² leaf area (Pereira et al., 1992).

SLA of new leaves was calculated as a function of foliar N:C ratio using an empirical relationship (Eq. (5)) derived from data for two *E. globulus* stands in the region (Fig. 2). This relationship, together with Eq. (8), produces a SLA of new foliage that declines from 9–11 m² kg⁻¹ for 1–2-year-old stands to 4–6 m² kg⁻¹ for stands between 6- and 10-year-old.

The plant production submodel was first parameterised under the assumption that N (and other nutrients) did not limit tree growth. This assumption seems reasonable given that soils were moderately fertile (Table 1) and nutrient concentrations in foliage and wood were relatively high (F. Hingston, unpublished data). Thus, leaf N:C ratio was set at its maximum and the soil decomposition submodel switched off. Model runs for each site covered a 10-year rotation period, starting at planting (age 0). Foliage, stem, branch/coarse roots and fine root biomass were set at appropriate initial values for young trees of a few months. At each site, initial available soil water was set at its maximum value, which is appropriate for simulations commencing in mid-winter when soils are relatively wet.

The C-allocation model was parameterised from leaf, stem and branch biomass, and height data from *E. globulus* stands aged 2–7 years (F.J. Hingston, unpublished data). We assumed dry sapwood density $\rho = 480$ kg DM m⁻³. The relationship between

observed leaf to sapwood area ratio (LS) and tree height (H), was used to parameterise Eqs. (10a)–(10c), giving $H_0 = 5$ m, $H_1 = 30$ m, $LS_0 = 8000$, $LS_1 = 2700$. Parameter values fitted to data on tree height versus stem mass (Eq. (11)) and branch mass versus stem mass (Eq. (14)) were: $b_1 = 4.8$, $b_2 = 0.35$, $b_3 = 5.61$ and $b_4 = 0.35$. Maximum leaf- and branch-allocation coefficients were set at $a_{f \max} = 0.33$ and $a_{b \max} = 0.40$, and root allocation was $a_r = 0.42$, 0.49 and 0.36 at Mumballup, Darkan and Northcliffe, respectively. The lack of root data makes it impossible to independently estimate parameters ϵ_0 and a_r . The value of $\epsilon_0 \times (1 - a_r)$ can be regarded as the maximum above-ground radiation-use efficiency. All other parameters in the plant production submodel were given empirically based values that were common to the three sites (excluding leaf litterfall parameters, see above, Table 2).

The model was able to reproduce observed tree growth data reasonably well at the three sites (Figs. 5 and 6). Simulated seasonal changes in LAI, resulting from decreased growth and enhanced leaf litterfall during summer, followed the observed patterns at Mumballup closely (RMSE = 0.27; $E = 0.9$). Model simulations overestimated LAI at Darkan ($E = -29$) and to a lesser extent at Northcliffe ($E = -7$). Our simulations are within the margin of error in LAI estimated by the LICOR-2000 plant canopy analyser, which underestimates LAI in discontinuous canopies (Fassnacht et al., 1994).

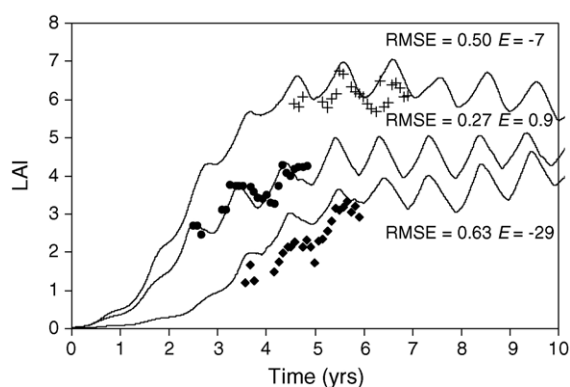


Fig. 5. Comparison of measured (symbols) and simulated (line) leaf area index (LAI) for *E. globulus* plantations at (●) Mumballup, (◆) Darkan and (+) Northcliffe. Simulations commenced 1st July 1988, 1st July 1987 and 1st July 1986 at Mumballup, Darkan and Northcliffe, respectively. Measured data are from Hingston et al. (1998). RMSE, root mean square error; E , relative error.

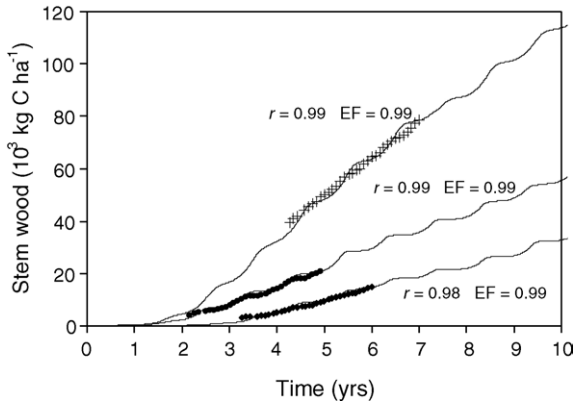


Fig. 6. Comparison of measured (symbols) and simulated (line) stemwood biomass for *E. globulus* plantations at (●) Mumballup, (◆) Darkan and (+) Northcliffe. Simulations commenced 1st July 1988, 1st July 1987 and 1st July 1986 at Mumballup, Darkan and Northcliffe, respectively. Measured data are from Hingston et al. (1998). r , coefficient of linear correlation between observed and simulated values; EF, model efficiency.

The rate of stem growth was simulated well at the three sites ($r=0.99$, 0.98 , 0.99 , respectively, for Mumballup, Darkan and Northcliffe and $EF=0.99$ for all three sites) (Fig. 6). Simulated stemwood productions showed a seasonal pattern that reflected seasonal change in soil moisture, but the simulated pattern was generally more pronounced than that observed.

4.4. Tree nitrogen cycling parameters

Values of most model parameters relating to tree N cycling were derived from measurements (Table 2). Data on N concentration in young, green leaves were available from *E. globulus* plantations of various ages. Fig. 7 shows the relationship of maximum N:C ratio of newly formed leaves ($n_{f\max 0}$) as a function of stand age (Eq. (8)) for $n_{f\max} = 0.066$, $n_{fM\max} = 0.022$ and $T_M = 6$ years, together with the observed data. Maximum N:C ratio of newly formed fine roots is kept constant with stand age (Table 2). For simplicity, the N:C ratios of branches and stems were assumed to be constant with stand age, and not dependent on N availability.

Nitrogen retranslocation from senescing leaves (t_f) and fine roots (t_r) are important model parameters because they have a large effect on the N content of the bulk plant litter. Nitrogen retranslocation determined

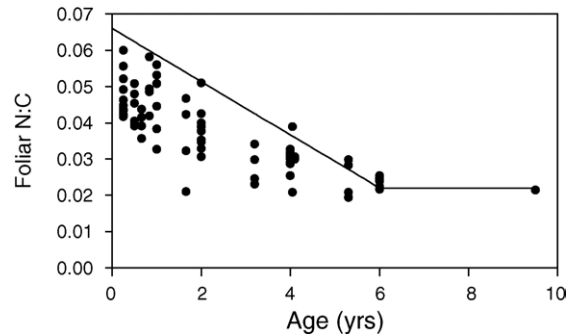


Fig. 7. Foliar N:C ratio of *E. globulus* stands as function of stand age. Experimental data (symbols) are from Cromer and Williams (1982), Judd et al. (1996), Bennett et al. (1997) and unpublished data from O'Connell, A.M. Line denotes the function for maximum foliar N:C ratio as adopted in the model.

from the difference between measured N concentrations in green and senesced foliage was 41, 52 and 41% at Mumballup, Darkan and Northcliffe, respectively (F.J. Hingston, unpublished data). These values are consistent with Sauer et al.'s (2000) values of 46–58% N retranslocated in young *E. globulus* trees. We assumed foliar retranslocation of 45% (Table 2) for all three sites. Precise information on N retranslocation in senescing fine roots is lacking because of methodological complications. Drawing upon data from a range of published studies, Gordon and Jackson (2000) concluded that mean N concentrations in live and dead fine roots were not significantly different, implying that there is little retranslocation of root N with senescence. We therefore set fine root N retranslocation (t_r) at zero (Table 2). Based on measured N concentrations in living and senesced branches, we assumed N retranslocation in branches (t_b) to be 50% (Table 2).

4.5. Decomposition submodel

We determined the biochemical composition of *E. globulus* leaf and branch litter by a proximate fractionation analysis (Table 3) and used these data to partition plant litter production into the different litter pools of the decomposition submodel. Since foliar litter consists of senescent tissues, its biochemical composition is different from foliar harvest residues which are mainly fresh green leaves. Other parameter values of the decomposition submodel were the same as those used when simulating mineralisation of euca-

Table 3
Biochemical composition of *E. globulus* leaf and branch litter determined by a proximate fractionation analysis (expressed on DM basis)

Litter type	Pools			Lignin (%)
	Metabolic (%)	Holocellulosic (%)	Ligno-cellulosic (%)	
Leaves	43	26	31	22
Fine roots	25	32	43	30
Branches	N/A	N/A	N/A	24

N/A, not applicable.

lypt harvest residues (see Table 1 in Corbeels et al., 2005b).

4.6. Initial soil C and N pools and soil N balance

Data on total soil C and N in the top 20-cm layer were available at the three sites (O'Connell and Rance, 1999) and are given in Table 1. The initial level of the microbial biomass pool was set at 0.8% of total SOM. This is a typical value for sandy soils under eucalypt plantations in south-western Australia (Mendham et al., 2002). The pools of *Young* and *Old* SOM in the decomposition submodel are defined on a conceptual basis (Corbeels et al., 2005b) and direct measurement of their size is problematic. Their initial values in the 0–20 cm top-soil layer at each site were, therefore, estimated by fitting the decomposition submodel to data on N mineralisation from respective soil samples (0–20 cm) incubated under controlled conditions (25 kPa, 20 °C) during a 220-day period. Table 4 shows the results of these fitting runs as ratios of *Young* C to total C and *Young* N to total N for the three sites. The soil at Darkan shows higher proportions of *Young* C and N compared to the other two sites, which means that soil N at this site is more readily mineralisable than at the other sites. This finding is in agreement with the results of the labile soil N analyses (Table 1).

Nitrogen input through atmospheric deposition was set at 8 kg N ha⁻¹ yr⁻¹ (O'Connell, 1985). Leaching and gaseous losses of N were not measured at the

Table 4
Initial values for *Young* soil C and N in model simulations at the three sites (expressed as % of total C and N, respectively)

Site	<i>Young</i> soil C (%)	<i>Young</i> soil N (%)
Mumballup	20	15
Darkan	40	40
Northcliffe	25	20

experimental sites. However, other experiments have indicated that losses of N through leaching under non-fertilised forest plantations on sandy soils in southern Australia are minimal (Carlyle, 1995), whilst the denitrification potential is low because anaerobic conditions rarely occur on sandy soils. We therefore assumed that no N losses occurred from the plant–soil system at the three sites.

5. Testing of the N mineralisation model

The model was then run as parameterised above with the decomposition submodel switched on. Nitrogen contents of tree biomass pools were calculated by balancing N inputs and losses from trees taking into account the maximum N:C ratios of each pool and retranslocation before senescence. Values for initial soil conditions, which are related to C and N status, were discussed above. Initial sizes of the various plant litter pools were set at zero.

Simulated annual rates of net N mineralisation from SOM (0–20 cm) and litter (both above- and below-ground) together with observed values in the top 20-cm soil layer (O'Connell and Rance, 1999) are presented in Fig. 8 for the three sites. We obtained N mineralisation in the top 20 cm soil layer by assuming it represents 80% of total N mineralised (Connell et al., 1995). Simulated annual rates of N mineralisation ranged from 51 to 94, 55 to 126 and 84 to 159 kg N ha⁻¹ yr⁻¹, at Mumballup, Darkan and Northcliffe, respectively. There was no obvious common trend with stand age. At Northcliffe simulated annual rate of N mineralisation peaked at age 3 years, at Mumballup highest rates were simulated at ages 3–5, whereas at Darkan N mineralisation was highest at age 5. Total model error as indicated by RMSE was highest for Darkan, followed by Mumballup and then Northcliffe. The negative *E* values for

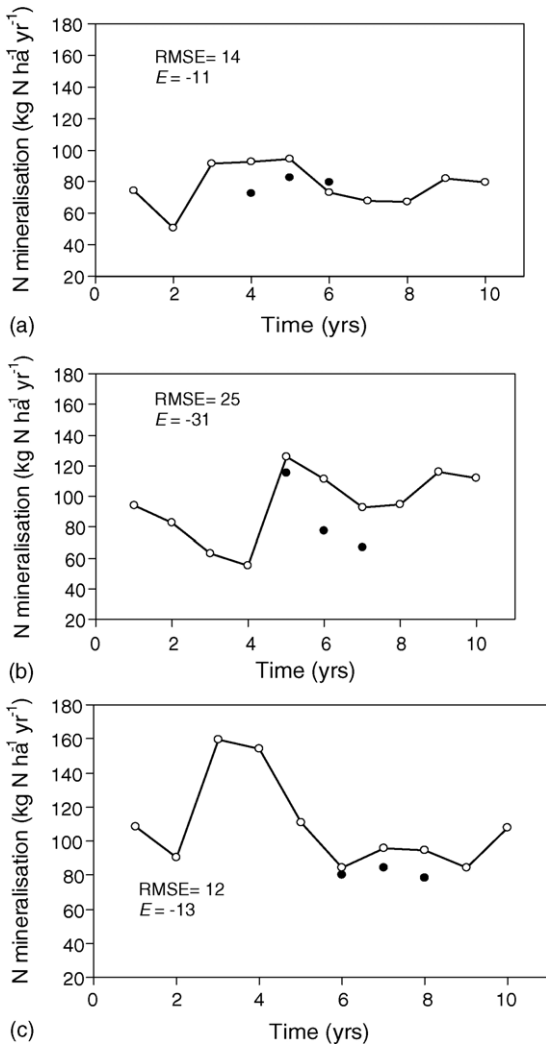


Fig. 8. Simulated (line/open symbols) and measured (solid symbols) annual rates of net soil N mineralisation for *E. globulus* plantations at (a) Mumballup, (b) Darkan and (c) Northcliffe. Simulations commenced 1st July 1988, 1st July 1987 and 1st July 1986 at Mumballup, Darkan and Northcliffe, respectively. Measured data are from O’Connell and Rance (1999). RMSE, root mean square error; *E*, relative error.

the three sites suggested an overall bias towards overestimation by the model. On three occasions (twice at Darkan and once at Mumballup) overestimation of more than 25% occurred.

Model output mirrored the seasonal pattern of measured N mineralisation, as shown for the Mumballup site in Fig. 9. Mineralisation rates were highest during

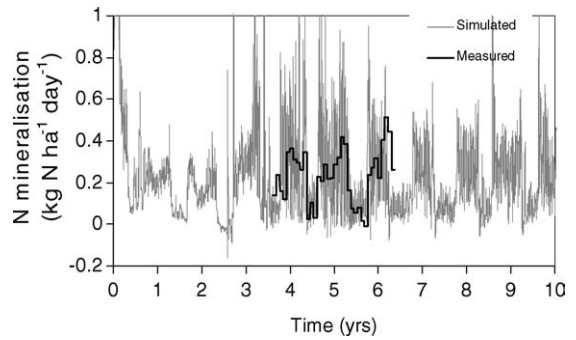


Fig. 9. Comparison of measured (black line) and simulated (grey line) daily net soil N mineralisation rates (0–20 cm) for the *E. globulus* plantation at Mumballup. Simulations of G’DAY commenced on 1st July 1988. Measured data are from O’Connell and Rance (1999) and are average daily rates over 28-day periods.

late winter and spring when soil moisture was not in deficit and soil temperature was rising. Rates were low in summer when the forest floor and top-soil dried out.

6. Sensitivity and identifiability analysis

In this section we report the results of a sensitivity and identifiability analysis applied to the model using the available soil water, LAI, leaf litterfall and stemwood measurements from the three sites. An identifiability analysis looks at the over-parameterisation of the model, and selects identifiable parameter subsets that can be validly fitted from the available measurements. We verified whether the 13 parameters (see Table 2) whose values were estimated through model fitting (henceforth referred to as the ‘fitted’ parameters), were identifiable. The formulae of this analysis are outlined in Brun et al. (2001) and Corbeels et al. (2005b).

Table 5 shows the 25 most sensitive model parameters in decreasing order of sensitivity, together with sensitivity values for the 13 ‘fitted’ parameters. The parameters related to C allocation in trees have the strongest overall contribution to variability in model output: 6 of the 10 most sensitivity parameters are from the C-allocation algorithm of the model. Besides, 8 of the 13 ‘fitted’ parameters belong to the 25 most sensitive parameters.

To be identifiable a parameter subset has to consist of sufficiently sensitive parameters and, secondly, sen-

Table 5

Parameter sensitivity ranking with respect to the four simulated variables: soil water content, LAI, leaf litterfall and stemwood at the three *E. globulus* sites

Rank	Parameter	δ_j^{msqr}
1	b_2	1.157
2	b_1	0.708
3	a_r	0.634
4	ε_o	0.482
5	H_1	0.454
6	c_{dm}	0.429
7	$W_{t\max}$	0.418
8	ρ	0.313
9	$a_{b\max}$	0.283
10	LS_1	0.240
11	r_s	0.220
12	$l_{f\max}$	0.199
13	α_{lab}	0.191
14	k_p	0.172
15	$FT_{w\max}$	0.169
16	b_4	0.163
17	σ_0	0.147
18	b_3	0.144
19	$FP_{w\text{crit}}$	0.140
20	σ_{\max}	0.134
21	LS_0	0.111
22	$FL_{w\max}$	0.104
23	$l_{f\min}$	0.099
24	$a_{f\max}$	0.095
25	L_{cc}	0.090
31	q_{et}	0.0469
33	δ_{LS}	0.0453
41	$FT_{w\min}$	0.0241
43	δ_{BS}	0.0178
50	λ_p	0.0152

Simulations were run for a 10-year period for each site. δ_j^{msqr} is root mean square sensitivity of the model output to a change in the parameter. Values of δ_j^{msqr} are based on daily outputs of each variable weighted by the mean simulated value of that variable over 10 years. For formula, see Appendix A in Corbeels et al. (2005b). Prior parameter uncertainty was set at 50% for all parameters.

sitivities of the parameters must not be approximately linearly dependent. To check the second condition collinearity indices, γ_K , are calculated for subsets of parameters, and parameter subsets showing a γ_K below a threshold of 10 are considered as potentially identifiable subsets (Brun et al., 2001). Results are given in Table 6. There are parameter subsets up to size 11 which fulfil $\gamma_K < 10$ (subsets no 6 in Table 6). Subsets of size 12 and higher have $\gamma_K > 10$. A maximum of 11 parameters is, therefore, considered as potentially identifiable from the available measurements. The seven most sen-

sitive ‘fitted’ parameters (subset no. 1) show a γ_K of 5.5, and are thus identifiable. Adding to this subset the 8th most sensitive ‘fitted’ parameter, L_{cc} , which represents the LAI corresponding to complete ground cover, causes severe identifiability problems (see subset no. 2 in comparison with subsets nos. 1 and 3). It means that a given model output could be obtained from different combinations of values of L_{cc} with those of the other parameters. A further analysis of subsets including the ten (subset no. 4) to eleven (subset no. 5) most sensitive parameters, but without L_{cc} , shows γ_K values approaching the threshold value of 10.

7. Discussion

7.1. Coupled plant–soil model

We have modified the original version of the G'DAY plant–soil model (Comins and McMurtrie, 1993) to simulate C and N cycling in fast-growing, short-rotation forest plantations. The new version of G'DAY was applied to three *E. globulus* stands in south-western Australia. We were able to correctly simulate the observed time-course of stemwood and LAI at all three sites (Figs. 5 and 6). With an a priori parameterisation of the decomposition submodel for *E. globulus* residues (see Corbeels et al., 2005b), the model was then used to predict soil N mineralisation rates at the three sites (Fig. 8).

This version of G'DAY represents the processes of plant N uptake, microbial N uptake and N loss in a similar way—i.e. their maximum rates are all proportional to soil inorganic N. The ratio $\lambda_p:\lambda_m$ (rate of plant N uptake: microbial N uptake) characterises the relative competitive abilities of trees and microorganisms for soil inorganic N. Experimental evidence for competition for N between plants and microorganisms comes from long and short-term experiments using ^{15}N . The identification of the key determinants of competitive advantage is, however, complex. Key determinants that are evident include spatial differences in N availability and in root and microbial distribution, together with temporal differences in microbial and root turnover (Hodge et al., 2000). A very feasible way forward to increase our understanding in this field would be to use the model to test different hypotheses – about competitive advantages between plants and

Table 6
Collinearity indices of selected parameter sets consisting of ‘fitted’ model parameters

Set no.	Set size	Parameters	γ_K
1	7	The seven most sensitive ‘fitted’ parameters: $a_r, a_{b\max}, l_{f\max}, FT_{w\max}, FL_{w\max}, l_{f\min}, a_{f\max}$	5.5
2	8	The eight most sensitivity ‘fitted’ parameters: $a_r, a_{b\max}, l_{f\max}, FT_{w\max}, FL_{w\max}, l_{f\min}, a_{f\max}, L_{cc}$	82.4
3	8	The nine most sensitive ‘fitted’ parameters excluding L_{cc} : $a_r, a_{b\max}, l_{f\max}, FT_{w\max}, FL_{w\max}, l_{f\min}, a_{f\max}, q_{et}$	9.3
4	9	The 10 most sensitive ‘fitted’ parameters excluding L_{cc} : $a_r, a_{b\max}, l_{f\max}, FT_{w\max}, FL_{w\max}, l_{f\min}, a_{f\max}, q_{et}, \delta_{LS}$	9.6
5	10	The 11 most sensitive ‘fitted’ parameters excluding L_{cc} : $a_r, a_{b\max}, l_{f\max}, FT_{w\max}, FL_{w\max}, l_{f\min}, a_{f\max}, q_{et}, \delta_{LS}, FT_{w\min}$	9.8
6a	11	The parameter subsets of size 11 with $\gamma_K < 10$: $a_r, l_{f\max}, FT_{w\max}, FL_{w\max}, l_{f\min}, a_{f\max}, q_{et}, \delta_{LS}, FT_{w\min}, \delta_{BS}, \lambda_p$	6.5
6b	11	$a_{b\max}, l_{f\max}, FT_{w\max}, FL_{w\max}, l_{f\min}, a_{f\max}, q_{et}, \delta_{LS}, FT_{w\min}, \delta_{BS}, \lambda_p$	6.6
6c	11	$l_{f\max}, FT_{w\max}, FL_{w\max}, l_{f\min}, a_{f\max}, L_{cc}, q_{et}, \delta_{LS}, FT_{w\min}, \delta_{BS}, \lambda_p$	6.6
6d	11	$a_r, l_{f\max}, FT_{w\max}, FL_{w\max}, l_{f\min}, a_{f\max}, L_{cc}, q_{et}, \delta_{LS}, FT_{w\min}, \lambda_p$	9.7
6e	11	$a_r, a_{b\max}, l_{f\max}, FT_{w\max}, FL_{w\max}, l_{f\min}, a_{f\max}, q_{et}, \delta_{LS}, FT_{w\min}, \lambda_p$	9.8
7	13	All 13 ‘fitted’ parameters: $a_r, a_{b\max}, l_{f\max}, FT_{w\max}, FL_{w\max}, l_{f\min}, a_{f\max}, L_{cc}, q_{et}, \delta_{LS}, FT_{w\min}, \delta_{BS}, \lambda_p$	86.9

γ_K : indicates the degree of linear dependence of normalised sensitivities to the parameter subset. For formula, see Appendix A in Corbeels et al. (2005b).

microorganisms for N – against existing experimental data.

7.2. Nitrogen mineralisation

Simulated annual rates of N mineralisation at the three sites in south-western Australia ranged from about 50–160 kg N ha⁻¹ (in the litter plus 0–20 cm soil layers, assumed to represent about 80% of total N mineralisation, Connell et al., 1995) and are the result of the interacting processes of litter production, SOM and litter decomposition, and microbial N immobilisation and (re-)mineralisation. Differences in temporal patterns of soil N mineralisation across the three sites are related to differences in temporal patterns and amounts of litterfall, and to differences in soil moisture status, which affects decomposition rate. As illustrated in Fig. 10 for the Mumballup site, the model output underlines a shift in the balance in source of N supply from SOM to plant litter. The contribution from SOM mineralisation to total N mineralisation decreases with stand age, while recycling N through mineralisation of litter (foliage and fine roots) becomes important fol-

lowing canopy closure, i.e. after about 3–4 years of tree growth. The model results also indicate that during the first 2 years of the rotation decomposing tree litter produces a small net N immobilisation. This implies that different factors affect N availability in young compared to established stands. For young trees, N supply is largely controlled by the size and decomposability of

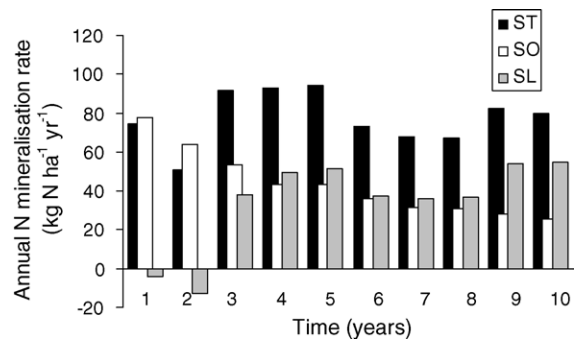


Fig. 10. Simulated rates of annual net soil N mineralisation for the *E. globulus* plantation at Mumballup. ST is simulated total N mineralisation, SO is simulated N mineralisation from soil organic matter, and SL is simulated N mineralisation from tree litter.

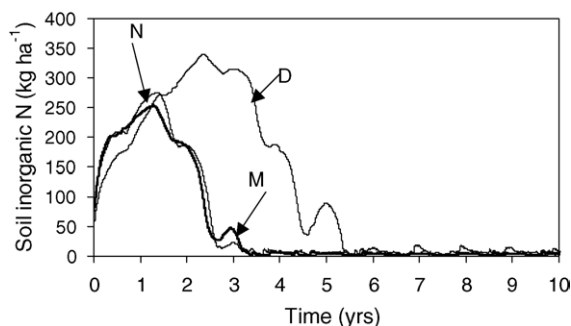


Fig. 11. Simulated soil inorganic N content in the root zone under *E. globulus* plantations at (M) Mumballup, (D) Darkan and (N) Northcliffe. Simulations commenced 1st July 1988, 1st July 1987 and 1st July 1986 at Mumballup, Darkan and Northcliffe, respectively. Simulations assume zero N loss.

native SOM, whereas for established stands the amount of litter produced during growth, its N:C ratio and its decomposability are important.

Initially, simulated levels of soil inorganic N are high under the growing plantation, while from about age 2 to 3 (depending on the site) soil inorganic N decreases and becomes depleted (Fig. 11). This is because, during the first years after planting, N mineralisation occurs faster than tree N uptake, whereas between about years 2 and 5 (depending on the site), when the trees are building their canopies, the tree demand for N equals or exceeds the N mineralisation rate. Consequently, plantations are most likely to respond to fertiliser N applications during the canopy building phase, with scope for optimising N supply for maximal productivity and minimal leaching. Moreover, the simulated levels of soil inorganic N emphasise a higher risk for N loss through leaching during the first few years just after planting the stand than later after N has been incorporated into plant tissues. This risk is likely to be heightened when N mineralisation is enhanced early in a rotation as a result of soil disturbance during planting operations (Vitousek and Matson, 1985). These hypotheses based on model simulations are in agreement with field observations under second-rotation eucalypt plantations in south-western Australia (O'Connell et al., 2004), showing that soil inorganic N accumulates early, during the first 2 years of the rotation, but decreases thereafter to low values.

The model results suggest that, depending on the rainfall conditions, a soil N supply of approxi-

mately 70–120 kg N ha⁻¹ yr⁻¹ (0–20 cm) is not limiting plantation productivity in south-western Australia (Figs. 8 and 10). The ability to predict N mineralisation in forest plantations and relate this to tree requirements for optimum productivity is a key element for describing soil nutrient effects on tree growth. It has often been difficult to show a relationship between soil biogeochemical properties and productivity of forests (Nambiar, 1995; Stape et al., 2004). The difficulty lies in the complexity of soil biogeochemistry per se and in the fact that growth rates are governed by the rate at which soil nutrients become available to trees, which is – in the case of N – determined by mineralisation. Predicting soil N mineralisation under short-rotation forest plantations is therefore valuable for efficient N management, allowing improved use of chemical fertilisers that may reduce N loss and minimise adverse environmental effects resulting from N leakage into other ecosystems. Simpler, empirical models based on a soil mineralisation index (e.g. O'Connell and Rance, 1999) have also proven to be effective practical tools for this purpose. However, these types of models have limited application because they are site-specific and do not account for temporal changes in N mineralisation during stand development as litter inputs change (Paul et al., 2002). On the other hand, G'DAY is responsive to distinct site conditions and management practices and able to capture the effects of interannual variations in precipitation and residue additions (Corbeels et al., 2005a). For use on other sites (and species), it will require, however, a degree of site (and species)-specific parameterisation and further testing. Once this done, it can then be used to evaluate impacts of factors such as drought or harvest residue management that affect N supply and plantation growth.

7.3. Fine root allocation and turnover

A great source of uncertainty in the above model simulations is the contribution to N mineralisation from fine roots. Simulations with altered rates of fine root turnover and N content can illustrate the importance of fine roots for N mineralisation and immobilisation. For example, if we halve both fine root turnover, l_r from 2.4 to 1.2 yr⁻¹ and the maximum fine root N:C ratio, $n_{r,max}$ from 0.017 to 0.0085 the model predicts (for the Mumballup site) a reduction in the annual rate of soil N mineralisation of about 75% during stand ages 3 and

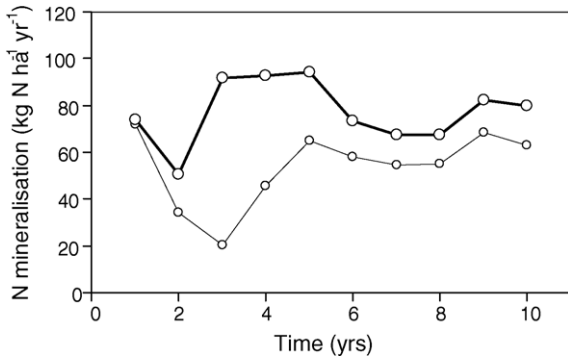


Fig. 12. Effect of changing parameters values for fine root turnover, l_r and maximum fine root N:C ratio, $n_{r,max}$ on simulated annual rate of net soil N mineralisation at Mumballup. Lines are outputs from model simulations over a 10-year eucalypt rotation with the site-specific input parameters and weather data (1988–1998) for the Mumballup site. (bold line) $l_r = 2.4 \text{ yr}^{-1}$ and $n_{r,max} = 0.017$; (fine line) $l_r = 1.2 \text{ yr}^{-1}$ and $n_{r,max} = 0.0085$.

4, which decreases to about 20% during later years (Fig. 12).

Measurements of (fine) root production and of their turnover are, however, experimentally difficult and data on fine root biomass (live and dead) are scarce. We have used an average ‘best available’ value (2.4 yr^{-1} , Table 2) for fine root turnover of *E. globulus* (Kätterer et al., 1995). The allocation coefficient for fine roots was set constant so that the ‘residual’ allocation coefficient for stems (Eq. (16)) fits stemwood biomass, given the leaf- and branch-allocation constraints (Eqs. (10a)–(10c) and (14)). Estimated allocation to fine roots ranged from 0.36 at Northcliffe to 0.49 at the Darkan site (Table 2), and is consistent with the hypothesis that C is allocated preferentially to fine roots if conditions limit the supply of water (or of nutrients) (Santantonio, 1989; Ruess et al., 1996; Nadelhoffer, 2000).

Because of the methodological difficulties in root research it is difficult to generalize about controls on fine root dynamics. Mechanistic models provide one option for exploring these processes. For example, Hendricks et al. (1993) hypothesised that soil N availability controls dynamics of fine roots in a way analogous to those of foliage. This would imply that absolute production and turnover of fine roots increases with N availability, a hypothesis that could be explored further using this new version of G'DAY, especially if data with N availability gradients are available.

7.4. Further model developments

There are mechanisms not accounted for in the model and some assumed relationships deserve more attention. In particular, the functional relationship between sapwood area and leaf area requires verification, and care should be taken when simulating long-term ecosystem responses to environmental change or to management practices. Allometric relationships may vary with site conditions and silvicultural treatments (cf. Medhurst et al., 1999). Environmental controls on biomass allocation in growing trees are not well understood (Cannell and Dewar, 1994; Lacoite, 2000). Forest ecosystem models (e.g. CABALA, Battaglia et al., 2004) that describe the process of biomass allocation in a way that adjusts allocation to the supply rates of resources are currently scarce.

It is desirable in models that each process is represented at a level of detail that is commensurate with the relative importance of that process (e.g. May, 2004). We have addressed this issue by analysing the model's sensitivity to specific parameters (Table 5). This analysis reveals that the model is most sensitive to several C-allocation parameters (e.g. b_1 , b_2 , a_r , H_1), and to the radiation-use efficiency (ϵ_0). In G'DAY, as in several other plant–soil models, this means that more emphasis should be given to modelling above- and below-ground allocation processes, including the relationship between (fine) root dynamics and soil resource availability. The sensitivity to ϵ_0 suggests that modelling of radiation-use efficiency is another area where the model could be improved in the future.

Other feedback mechanisms between N availability and plant production that have not been fully included in this version of G'DAY, but that will need careful consideration are N controls on leaf and fine root longevity, substrate quality, and N retranslocation efficiencies during senescence. Several studies suggest that there are strong feedbacks between N availability and the quality of litter produced (for leaves and for fine roots, see Hendricks et al., 2000). In our model, a feedback loop of N availability on litter quality is present through changed N:C ratios of litter pools. However, it is also possible that as N availability decreases, leaves and fine roots have higher concentrations of ‘recalcitrant’ compounds such as lignin (Hendricks et al., 2000). This phenomenon, coupled with increased leaf and fine root longevity and increased N retranslocation efficiency

during senescence may result in less readily decomposable litter, further decreasing site N availability, and thereby completing a negative feedback for the system.

Finally, we assumed in G'DAY that neither plant nor the microbial organisms is capable of direct uptake of organic N. This hypothesis is indirectly supported for plants by a close relationship between net N mineralisation rates and plant N uptake in some ecosystems, and has been widely accepted in agronomy and ecology. Recent research findings (see Kay and Hart, 1997) however point to the potential importance of uptake of significant amounts of organic N by plant mycorrhizal associations. Such a development should perhaps be incorporated into the model.

8. Conclusions

The updated version of G'DAY, which allows the simulation of C and N cycling in fast-growing forest plantations, was parameterised for *E. globulus* using available data on soil water content, LAI, leaf litter-fall and stem growth from three sites in south-western Australia. Model output is most sensitivity to parameters that relate to the calculation of C allocation in trees. The model – with an a priori parameterisation of the decomposition submodel – was then used to predict soil N mineralisation rates under the three stands. The simulated rates of soil N mineralisation of 50–160 kg N ha⁻¹ yr⁻¹ tended to overestimate observed values. The model simulations also indicated the importance of fine root production and turnover for N supply. More knowledge on fine root dynamics is needed for further model development and testing.

On the whole, the results of this study suggest that, the major feedbacks associated with litter production, organic matter decomposition and N availability are adequately integrated in G'DAY. The G'DAY model provides, hence, a useful framework for evaluating management options for sustainable forest plantation productivity and for analysing constraints on long-term productivity and C storage.

Acknowledgements

This work was supported by the Australian Centre for International Agricultural Research (ACIAR).

Ross McMurtrie and David Pepper acknowledge financial support from the Australian Research Council and the Australian Greenhouse Office. We also thank two anonymous reviewers for comments that helped improve this manuscript.

Appendix A

See Table A.1.

Table A.1
Symbols, description and units for model variables and parameters

Symbol	Description
a_b, a_f, a_r, a_s	Branches, leaf, fine root and stem allocation coefficients
$a_{b\max}, a_{f\max}$	Maximum branch and leaf allocation coefficients
A_{imm}	Flux of abiotic or chemical N immobilisation in Young SOM (kg N m ⁻² yr ⁻¹)
a_N	Constant determining the relationship between critical foliar N:C ratio ($n_{f\text{crit}}$) and maximum leaf N:C ratio ($n_{f\text{max}}$)
A_s	Stem sapwood cross-sectional area (m ² m ⁻² ground)
b_1, b_2	Constant and exponent in tree height–stemwood mass relationship
b_3, b_4	Constant and exponent in branch–stemwood mass relationship
b_{ff}, b_s	Reduction factors on evaporation from forest floor litter and top-soil layer for reduced moisture
$C_b, C_f, C_h, C_r, C_s, C_w$	C mass of branches, foliage, heartwood, fine roots, sapwood and stemwood (kg C m ⁻²)
c_{dm}	Carbon content of plant DM (g C g ⁻¹ DM)
E_{ff}, E_{top}	Daily evaporation rate from forest floor litter and top-soil layers (mm day ⁻¹)
E_o	Daily potential evaporation rate (mm day ⁻¹)
$D_{ff}, D_{\text{sub}}, D_{\text{top}}$	Daily drainage rate out of forest floor litter, sub- and top-soil layer (mm day ⁻¹)
f_L	Reduction of NPP as function of absorbed PAR
f_N	Reduction of NPP as function of leaf N:C ratio
f_W	Reduction of NPP as function of PAW
FP_{wcrit}	Fractional PAW below which NPP is function of PAW
$FL_{\text{wmax}}, FL_{\text{wmin}}$	Fractional PAW above which foliar litterfall rate is at its minimum, and below which foliar litterfall rate is at its maximum
$FT_{\text{wmax}}, FT_{\text{wmin}}$	Fractional PAW above which transpiration rate is at its maximum, and below which transpiration is zero
G_c	Fractional ground cover
H	Average tree height (m)

Table A.1 (Continued)

Symbol	Description
H_0, H_1	Tree height when the ratio of projected leaf area index to stem sapwood cross-sectional area is, respectively, LS_0 and LS_1
I_a	Absorbed PAR ($MJ m^{-2} yr^{-1}$)
I_o	Incident PAR ($MJ m^{-2} yr^{-1}$)
k_p	PAR extinction coefficient
k_t	Total radiation extinction coefficient
L	LAI
l_b, l_f, l_r, l_s, l_h	Litterfall rates of branches, leaves, fine roots, sapwood and heartwood (yr^{-1})
L_{cc}	LAI of closed canopy
l_{fmax}, l_{fmin}	Maximum and minimum foliage litterfall rates (yr^{-1})
LS	The ratio of projected leaf area to stem sapwood cross-sectional area
LS_0, LS_1	The ratio of projected leaf area to stem sapwood cross-sectional area when tree height is, respectively, H_0 and H_1
n_b, n_{nw}, n_{sw}	N:C ratios of branches, non-structural and structural wood
n_f	N:C ratio of leaves
n_{fcrit}	Critical foliar N:C ratio below which NPP is function of leaf N:C ratio
n_{fmax0}	Maximum N:C ratio of newly formed leaves
n_{fMmax}	Maximum N:C ratio of newly formed leaves at mature stand age, T_M
n_{fYmax}	Maximum N:C ratio of newly formed leaves at stand age 0
N_{imm}	Gross N immobilisation flux ($kg N m^{-2} yr^{-1}$)
N_{in}	External N input flux (from deposition, biological fixation and chemical fertiliser) to soil inorganic N pool ($kg N m^{-2} yr^{-1}$)
N_{inorg}	Soil inorganic N pool ($kg N m^{-2}$)
N_{loss}	N loss flux (through leaching or gaseous emissions) from soil inorganic N pool ($kg N m^{-2} yr^{-1}$)
N_{min}	Gross N mineralisation flux ($kg N m^{-2} yr^{-1}$)
n_{rmax}	Maximum N:C ratio of newly formed fine roots
P_n	Net primary production ($kg C m^{-2} yr^{-1}$)
q_{et}	Fraction of tree water uptake from top-soil layer
R_{eff}	Daily effective rainfall ($mm day^{-1}$)
R_n	Net radiation ($J m^{-2} day^{-1}$)
r_s	Sapwood to heartwood turnover rate (yr^{-1})
s	Slope of the saturation vapour pressure–temperature curve ($Pa ^\circ C^{-1}$)
t_b, t_f, t_r	Fraction of N in branches, leaves and fine roots retranslocated before senescence
T_M	Age of mature stand (yr)
T_{sub}, T_{top}	Daily transpiration rate from sub- and top-soil layers ($mm day^{-1}$)
T_t	Daily total transpiration rate ($mm day^{-1}$)
U_p	Flux of N uptake by plants ($kg N m^{-2} yr^{-1}$)

Table A.1 (Continued)

Symbol	Description
W_{ff}, W_{sub}, W_{top}	Plant available water in forest floor litter, sub- and top-soil layers (mm)
$W_{ffmax}, W_{topmax}, W_{tmax}$	Maximum amounts of plant available water in forest floor litter, top-soil layer and total root zone (mm)
W_t	Total plant available water (mm)
α_{lab}	Labile fraction of microbial biomass
δ_{BS}	Parameter characterises the variability in a_b and a_w
δ_{LS}	Parameter representing the variability in a_f and a_w
γ	Psychometric constant ($Pa ^\circ C^{-1}$)
ϵ_o	Maximum PAR utilisation efficiency ($kg DM MJ^{-1}$)
λ	Latent heat of water vaporisation ($J kg^{-1}$)
λ_l	Rate of loss from inorganic N pool (yr^{-1})
λ_m	Potential rate of microbial N uptake from inorganic N pool (yr^{-1})
λ_p	Potential rate of plant N uptake from inorganic N pool (yr^{-1})
ρ	Sapwood density ($kg m^{-3}$)
σ	Specific leaf area ($m^2 kg^{-1}$)
σ_0	Specific leaf area of newly formed foliage ($m^2 kg^{-1}$)
σ_{max}	Maximum specific leaf area of newly formed foliage ($m^2 kg^{-1}$)

Abbreviations: C, carbon; DM, dry matter; LAI, leaf area index; N, nitrogen; NPP, net primary productivity; PAR, photosynthetically active radiation; PAW, plant available water; SOM, soil organic matter. **Subscripts:** b, branch (including coarse roots); f, foliage; ff, forest floor; h, heartwood; r, fine root; s, sapwood; sub, sub-soil layer; top, top-soil layer; w, stemwood. For values of parameters, see Tables 1 and 2.

References

- Aber, J.D., Melillo, J.M., Federer, C.A., 1982. Predicting the effects of rotation length, harvest intensity and fertilization on fiber yield from northern hardwood forests in New England. *For. Sci.* 28, 31–45.
- Addiscott, T.M., Whitmore, A.P., 1987. Computer simulation of changes in soil mineral nitrogen and crop nitrogen during autumn, winter and spring. *J. Agric. Sci. Camb.* 109, 141–157.
- Agus, C., Karyanto, O., Kita, S., Haibara, K., Toda, H., Hardinoto, S., Supriyo, H., Na'iem, M., Wardana, W., Sipayung, M.S., Khomsatun Wijoyo, S., 2004. Sustainable site productivity and nutrient management in a short rotation plantation of *Gmelina arborea* in east Kalimantan, Indonesia. *New For.* 28, 277–285.
- Almeida, A.C., Landsberg, J.J., Sands, P.J., 2004. Parameterisation of 3-PG model for fast-growing *Eucalyptus grandis* plantations. *For. Ecol. Manage.* 193, 179–195.

- Aronsson, P.G., Bergstrom, L.F., Elowson, S.N.E., 2000. Long-term influence of intensively cultured short-rotation Willow Coppice on nitrogen concentrations in groundwater. *J. Environ. Manage.* 58, 135–145.
- Battaglia, M., Sands, P., White, D., Mummery, D., 2004. CABALA: a linked carbon, water and nitrogen model of forest growth for silvicultural decision support. *For. Ecol. Manage.* 193, 251–282.
- Bauhus, J., Khanna, P.K., Menden, N., 2000. Aboveground and belowground interactions in mixed plantations of *Eucalyptus globulus* and *Acacia mearnsii*. *Can. J. For. Res.* 30, 1886–1894.
- Beadle, C.L., Honeysett, J.L., Turnbull, C.R.A., White, D.A., 1995. Site limits to achieving genetic potential. In: B.M. Potss, N.M.G. Borralho, J.B. Reid, W.N. Tibbits, C.A. Raymond (Eds.), *Eucalypt Plantations, Improving Fibre Yield and Quality*, Proc. CRCTHF-IUFRO Conference Hobart, 19–24 February 1995. CRC for Temperate Hardwood Forestry, Hobart, pp. 325–331.
- Bennett, L.T., Weston, C.J., Attiwill, P.M., 1997. Biomass, nutrient content and growth response to fertilisers of six-year-old *Eucalyptus globulus* plantations at three contrasting sites in Gippsland, Victoria. *Aust. J. Bot.* 45, 103–121.
- Bernhard-Reversat, F., 1996. Nitrogen cycling in tree plantation grown on a poor sandy savannah soil in Congo. *Appl. Soil Ecol.* 4, 161–172.
- Brun, R., Reichert, P., Künsch, H.R., 2001. Practical identifiability analysis of large environmental simulation models. *Water Resour. Res.* 37, 1015–1030.
- Campbell, J.L., Gower, S.T., 2000. Detritus production and soil N transformations in old-growth eastern hemlock and sugar maple stands. *Ecosystems* 3, 185–192.
- Cannell, M.G.R., Dewar, R.C., 1994. Carbon allocation in trees—a review of concepts for modeling. *Adv. Ecol. Res.* 25, 59–104.
- Carlyle, J.C., 1995. Nutrient management in a *Pinus radiata* plantation after thinning: the effect of thinning and residues on nutrient distribution, mineral nitrogen fluxes, and extractable phosphorus. *Can. J. For. Res.* 25, 1278–1291.
- Comins, H.N., McMurtrie, R.E., 1993. Long-term response of nutrient-limited forests to CO₂ enrichment: equilibrium behavior of plant–soil models. *Ecol. Appl.* 3, 666–681.
- Connell, M.J., Raison, R.J., Khanna, P.K., 1995. Nitrogen mineralization in relation to site history and soil properties for a range of Australian forest soils. *Biol. Fert. Soils* 20, 213–220.
- Corbeels, M., McMurtrie, R.E., Pepper, D.A., Mendham, D.S., Grove, T.S., O'Connell, A.M., 2005a. Long-term changes in productivity of eucalypt plantations under different harvest residue and nitrogen management practices: a modelling analysis. *For. Ecol. Manage.* 217, 1–18.
- Corbeels, M., McMurtrie, R.E., Pepper, D.A., O'Connell, A.M., 2005b. A process-based model of nitrogen cycling in forest plantations. I. Structure, calibration and analysis of the decomposition model. *Ecol. Modell.* 187, 426–448.
- Cromer, R.N., Williams, E.R., 1982. Biomass and nutrient accumulation in a planted *E. globulus* (Labill.) fertilizer trial. *Aust. J. Bot.* 30, 265–278.
- Dewar, R.C., 1993. A root-shoot partitioning model based on carbon–nitrogen–water interactions and Münch phloem flow. *Funct. Ecol.* 7, 356–368.
- Dewar, R.C., Medlyn, B.E., McMurtrie, R.E., 1998. A mechanistic analysis of light and carbon use efficiencies. *Plant Cell Environ.* 21, 573–588.
- Dewar, R.C., Medlyn, B.E., McMurtrie, R.E., 1999. Acclimation of the respiration photosynthesis ratio to temperature: insights from a model. *Glob. Change Biol.* 5, 615–622.
- Dunin, F.X., 2002. Integrating agroforestry and perennial pastures to mitigate water logging and secondary salinity. *Agric. Water Manage.* 53, 259–270.
- Fabião, A., Madeira, M., Steen, E., Kätterer, T., Ribeiro, C., Araújo, C., 1995. Development of root biomass in an *Eucalyptus globulus* plantation under different water and nutrient regimes. *Plant Soil* 168–169, 215–223.
- Fassnacht, K.S., Gower, S.T., Norman, J.M., McMurtrie, R.E., 1994. A comparison of optical and direct methods for estimating foliage surface area index in forests. *Agric. For. Meteorol.* 71, 183–207.
- Gordon, W.S., Jackson, R.B., 2000. Nutrient concentrations in fine roots. *Ecology* 81, 275–280.
- Halliday, J.C., Tate, K.R., McMurtrie, R.E., Scott, N.A., 2003. Mechanisms for changes in soil C storage with pasture to *Pinus radiata* land-use change. *Glob. Change Biol.* 9, 1294–1308.
- Hendricks, J.J., Aber, J.D., Nadelhoffer, K.J., Hallett, R.D., 2000. Nitrogen controls on fine root substrate quality in temperate forest ecosystems. *Ecosystems* 3, 57–69.
- Hendricks, J.J., Nadelhoffer, K.J., Aber, J.D., 1993. Assessing the role of fine roots in carbon and nutrient cycling. *Trends Ecol. Evol.* 8, 174–178.
- Hingston, F.J., Galbraith, J.H., 1998. Application of the process-based model BIOMASS to *Eucalyptus globulus* ssp. *globulus* plantations on ex-farmland in south western Australia. II. Stemwood production and seasonal growth. *For. Ecol. Manage.* 106, 157–168.
- Hingston, F.J., Galbraith, J.H., Dimmock, G.M., 1998. Application of the process-based model BIOMASS to *Eucalyptus globulus* ssp. *globulus* plantations on ex-farmland in south western Australia. I. Water use by trees and assessing risk of losses due to drought. *For. Ecol. Manage.* 106, 141–156.
- Hodge, A., Robinson, D., Hodge, A.F., 2000. Are microorganisms more effective than plants at competing for nitrogen? *Trends Plant Sci.* 5, 304–308.
- Jackson, J.E., Palmer, J.W., 1981. Light distribution in discontinuous canopies: calculation of leaf areas and canopy volumes above defined 'irradiance contours' for use in productivity modelling. *Ann. Bot.* 47, 561–565.
- Judd, T.S., Bennett, L.T., Weston, C.J., Attiwill, P.M., Whiteman, P.H., 1996. The response of growth and foliar nutrients to fertilizers in young *Eucalyptus globulus* (Labill.) plantations in Gippsland, southeastern Australia. *For. Ecol. Manage.* 82, 87–101.
- Kätterer, T., Fabião, A., Madeira, M., Ribeiro, C., Steen, E., 1995. Fine-root dynamics, soil moisture and soil carbon content in a *Eucalyptus globulus* plantation under different irrigation and fertilization regimes. *For. Ecol. Manage.* 74, 1–12.
- Kay, J.P., Hart, S.C., 1997. Competition for nitrogen between plants and soil microorganisms. *Trends Ecol. Evol.* 12, 139–143.
- Keith, H., Raison, R.J., Jacobsen, K.L., 1997. Allocation of carbon in a mature eucalypt forest and some effects of soil phosphorus availability. *Plant Soil* 196, 81–99.

- King, D.A., 1996. A model to evaluate factors controlling growth in *Eucalyptus* plantations of southeastern Australia. *Ecol. Modell.* 87, 181–203.
- Laclau, J.-P., Ranger, J., Nzila, J.D., Bouillet, J.-P., Deleporte, P., 2003. Nutrient cycling in a clonal stand of *Eucalyptus* and an adjacent savanna ecosystem in Congo. 2. Chemical composition of soil solutions. *For. Ecol. Manage.* 180, 527–544.
- Lacointe, A., 2000. Carbon allocation among tree organs: a review of basic processes and representation in functional-structural tree models. *Ann. For. Sci.* 57, 521–533.
- Landsberg, J.J., Waring, R.H., 1997. A generalised model of forest productivity using simplified concepts of radiation-use efficiency, carbon balance and partitioning. *For. Ecol. Manage.* 95, 209–228.
- Landsberg, J.J., Waring, R.H., Coops, N.C., 2003. Performance of the forest productivity model 3-PG applied to a wide range of forest types. *For. Ecol. Manage.* 172, 199–214.
- Linder, S., 1985. Potential and actual production in Australian forest stands. In: Landsberg, J.J., Parsons, W. (Eds.), *Research for Forest Management*. CSIRO, Melbourne, pp. 11–35.
- Loague, K., Green, R.E., 1991. Statistical and graphical methods for evaluating solute transport models: overview and application. *J. Contam. Hydrol.* 7, 51–73.
- Magnani, F., Mencuccini, M., Grace, J., 2000. Age-related decline in stand productivity: the role of structural acclimation under hydraulic constraints. *Plant Cell Environ.* 23, 251–263.
- Mäkelä, A., Hari, P., 1986. Stand growth model based on carbon uptake and allocation in individual trees. *Ecol. Modell.* 33, 205–229.
- Mäkelä, A., Landsberg, J.J., Ek, A.R., Burk, E.T., Ter-Mikaelian, M., Ågren, G.I., Oliver, C.D., Puttonen, P., 2000. Process-based models for forest ecosystem management: current state of the art and challenges for practical implementation. *Tree Physiol.* 20, 289–298.
- May, R.M., 2004. Uses and abuses of mathematics in biology. *Science* 303, 790–793.
- McMurtrie, R.E., 1991. Relationship of forest productivity to nutrient and carbon supply: a modeling analysis. *Tree Physiol.* 9, 87–99.
- McMurtrie, R.E., Wolf, L., 1983. Above- and below-ground growth of forest stands: a carbon budget model. *Ann. Bot.* 52, 437–448.
- McMurtrie, R.E., Gholz, H.L., Linder, S., Gower, S.T., 1994. Climatic factors controlling the productivity of pine stands: a model-based analysis. In: Gholz, H.L., Linder, S., McMurtrie, R.E. (Eds.), *Environmental Constraints on the Structure and Productivity of Pine Forest Ecosystems: A Comparative Analysis*, Ecological Bulletins, Munksgaard International Booksellers and Publishers, Copenhagen, vol. 43, pp. 173–188.
- McMurtrie, R.E., Medlyn, B.E., Dewar, R.C., 2001. Increased understanding of nutrient immobilisation in soil organic matter is critical for predicting the carbon sink strength of forest ecosystems over the next 100 years. *Tree Physiol.* 21, 831–839.
- McMurtrie, R.E., Rook, D.A., Kelliher, F.M., 1990. Modelling the yield of *Pinus radiata* on a site limited by water and nitrogen. *For. Ecol. Manage.* 30, 381–413.
- Medhurst, J.L., Battaglia, M., Cherry, M.L., Hunt, M.A., White, D.A., Beadle, C.L., 1999. Allometric relationships for *Eucalyptus nitens* (Deane and Maiden) Maiden plantations. *Trees* 14, 91–101.
- Medlyn, B.E., McMurtrie, R.E., Dewar, R.C., Jefferys, M.P., 2000. Soil processes dominate the long-term response of forest net primary productivity to increased temperature and atmospheric CO₂ concentration. *Can. J. For. Res.* 30, 873–888.
- Mendham, D.S., O'Connell, A.M., Grove, T.S., 2002. Organic matter characteristics under native forest, long-term pasture, and recent conversion to *Eucalyptus* plantations in Western Australia: microbial biomass, soil respiration, and permanganate oxidation. *Aust. J. Soil Res.* 40, 859–872.
- Murty, D., McMurtrie, R.E., 2000. The decline of forest productivity as stands age: a model-based method for analysing causes for the decline. *Ecol. Modell.* 134, 185–200.
- Nadelhoffer, K.J., 2000. The potential effects of nitrogen deposition on fine-root production in forest ecosystems. *New Phytol.* 147, 131–139.
- Nambiar, E.K.S., 1995. Relationships between water, nutrients and productivity in Australian forests: application to wood production and quality. *Plant Soil* 168–169, 427–435.
- O'Connell, A.M., 1985. Nutrient accessions to the forest floor in karri (*Eucalyptus diversicolor* F. Muell.) forests of varying age. *For. Ecol. Manage.* 10, 283–296.
- O'Connell, A.M., Rance, S.J., 1999. Predicting nitrogen supply in plantation eucalypt forests. *Soil Biol. Biochem.* 31, 1943–1951.
- O'Connell, A.M., Grove, T.S., Mendham, D.S., Corbeels, M., McMurtrie, R.E., Shammass, K., Rance, S.J., 2004. Impact of inter-rotation site management on nutrient stores and flux rates and tree growth of Eucalypt plantations in south-western Australia. In: Nambiar, E.K.S., Ranger, J., Tiarks, A., Toma, T. (Eds.), *Site Management and Productivity of Tropical Plantation Forests*. CIFOR, Bogor, pp. 77–91.
- Parton, W.J., Schimel, D.S., Cole, C.V., Ojima, D.S., 1987. Analysis of factors controlling soil organic matter levels in Great Plains grasslands. *Soil Sci. Soc. Am. J.* 51, 1173–1179.
- Parton, W.J., Scurlock, J.M.O., Ojima, D.S., Gilmanov, T.G., Scholes, R.J., Schimel, D.S., Kirchner, T., Menaut, J.-C., Seastedt, T., Garcia Moya, E., Kamnalrut, A., Kinyamario, J.I., 1993. Observations and modeling of biomass and soil organic matter dynamics for the grassland biome worldwide. *Glob. Biogeochem. Cycl.* 7, 785–809.
- Paul, K.I., Polglase, P.J., O'Connell, A.M., Carlyle, J.C., Smethurst, P.J., Khanna, P.K., 2002. Soil nitrogen availability predictor (SNAP): a simple model for predicting mineralisation of nitrogen in forest soils: predicting nitrogen mineralisation of forests soils. *Aust. J. Soil Res.* 40, 1011–1026.
- Pepper, D.A., Del Grosso, S.J., McMurtrie, R.E., Parton, W.J., 2005. Simulated carbon sink response of shortgrass steppe, tall-grass prairie and forest ecosystems to rising [CO₂], temperature and nitrogen input. *Glob. Biogeochem. Cycl.* 19, GB1004, doi:10.1029/2004GB002226.
- Pereira, J.S., Chaves, M.M., Fonseca, F., Araujo, M.C., Torres, F., 1992. Photosynthetic capacity of leaves of *Eucalyptus globulus* (Labill.) growing in the field with different nutrient and water supplies. *Tree Physiol.* 11, 381–389.
- Ritchie, J.T., 1972. Model for predicting evaporation from a row crop with incomplete cover. *Water Resour. Res.* 8, 1204–1213.

- Rolff, C., Ågren, G.I., 1999. Predicting effects of different harvesting intensities with a model of nitrogen limited forest growth. *Ecol. Modell.* 118, 193–211.
- Ruess, R.W., Van Cleve, K., Yarie, J., Viereck, L.A., 1996. Contributions of fine root production and turnover to the carbon and nitrogen cycling in taiga forests of the Alaskan interior. *Can. J. For. Res.* 26, 1326–1336.
- Ryan, M.G., Hunt Jr., E.R., McMurtrie, R.E., Ågren, G.I., Aber, J.D., Friend, A.D., Rastetter, E.B., Pulliam, W.M., Raison, R.J., Linder, S., 1996. Comparing models of ecosystem function for temperate conifer forests. I. Model description and validation. In: Breymeyer, A.I., Hall, D.O., Melillo, J.M., Ågren, G.I. (Eds.), *SCOPE 56-Global Change: Effects on Coniferous Forests and Grasslands*. Wiley, Chichester, pp. 313–362.
- Sands, P.J., Landsberg, J.J., 2002. Parameterisation of 3-PG for plantation grown *Eucalyptus globulus*. *For. Ecol. Manage.* 163, 273–292.
- Sands, P.J., Battaglia, M., Mummery, D., 2000. Application of process-based models to forest management: PROMOD, a simple plantation productivity model. *Tree Physiol.* 20, 383–392.
- Santantonio, D., 1989. Dry-matter partitioning and fine-root production in forests: new approaches to a difficult problem. In: Pereira, J.S., Landsberg, J.J. (Eds.), *Biomass Production by Fast-growing Trees*. Kluwer Academic Publishers, Dordrecht, The Netherlands, pp. 57–72.
- Sauer, E., Nambiar, E.K.S., Fife, D.N., 2000. Foliar nutrient retranslocation in *Eucalyptus globulus*. *Tree Physiol.* 20, 1105–1112.
- Scott, N.A., Binkley, D., 1997. Foliage litter quality and annual net N mineralization: comparison across North American forest sites. *Oecologia (Berlin)* 111, 151–159.
- Slabbers, P.J., 1980. Practical prediction of actual evapotranspiration. *Irrig. Sci.* 1, 185–196.
- Smethurst, P., Holz, G., Moroni, M., Baillie, C., 2004. Nitrogen management in *Eucalyptus nitens* plantations. *For. Ecol. Manage.* 193, 63–80.
- Stape, J.L., Binkley, D., Ryan, M.G., 2004. Eucalyptus production and the supply, use and efficiency of use of water, light and nitrogen across a geographic gradient in Brazil. *For. Ecol. Manage.* 193, 17–31.
- Thornley, J.H.M., Johnson, I.R., 1990. *Plant and Crop Modelling*. Clarendon Press, Oxford, 669.
- Vitousek, P.M., Matson, P.A., 1985. Disturbance, nitrogen availability, and nitrogen losses in an intensively managed loblolly pine plantation. *Ecology* 66, 1360–1376.
- Waring, R.H., Landsberg, J.J., Williams, M., 1998. Net primary production of forests: a constant fraction of gross primary production? *Tree Physiol.* 18, 129–134.